Chapter 4. Sedimentology and Physical Volcanology

4.1. Materials and methods

In addition to the eight stratigraphic columns (Appendix 4) which were already measured and presented in the chapter before (see Fig. 5), and which will be more analysed in detail now, 20 2D-panels where obtained to study the complex interaction of fluvial, eruptive and mass flow processes from outcrop to landscape scale. 2D-panels were constructed at small scales (five, each ~ 800 m^2), medium scales (eight, each ~ 5000 m^2) and large scales (seven, each ~ 2 km^2), combined to a lithofacies model. Small scale panels describe the variety of different lithofacies types, interfingering in small areas, and the multitude of depositional processes involved in limited time and space. Medium scale panels show sedimentary trends and possible allocyclic patterns and finally, large scale panels document changes in the depositional system. The small scale panels and a part of the medium scale panels were already described by Trauth (2007) and included for interpretation.

The sedimentological analysis is based on the classification of lithofacies types and depositional elements, as well as measurements of natural gamma ray emission and magnetic susceptibility. The latter, however, did not provide satisfying results and will thus not be described more explicitly in this work. Vertical and lateral distribution of depositional elements together with stratigraphical data were used to reconstruct the evolution of the depositional environment within time, to identify volcanic centres, and to decipher cyclic patterns of volcanic and fluvial processes and process-coupling, e.g. increased debris flow activity after paroxysmal eruptions and the establishment of a braided river system in times of reduced volcanic activity. In addition, more than 200 palaeocurrent indicators (AMS and sedimentological features such as channel-wall orientations and trough cross-stratification directions) were measured to constrain dispersal patterns.

One problem in the investigation of pyroclastic flow deposits is the determination of its source vent locations. This problem, as well as the provenance of fluvial deposits, was solved by the application of studies on the magnetic susceptibility. The anisotropy of magnetic susceptibility (AMS) is a relatively fast and inexpensive method that yields three-dimensional flow markers (Cañón-Tapia and Castro, 2004). The susceptibility depends on the rock's minerals and their relative amounts, and is mainly related to the magma chemistry and crystallization conditions (Zanella et al., 1999). The AMS gives information on the spatial arrangement of ferromagnetic grains, i.e. the fabric, which relates to the emplacement forces. In lava flows, the fabric is mainly related to the flowage and is acquired before complete solidification, at temperatures higher than the Curie or Néel point of ferromagnetic minerals, marking the beginning of remanence acquisition (670 and 575°C, respectively for the Fe end-member of the titanohaematite and titanomagnetite series; Zanella et al., 1999).

The behaviour of pyroclastic rocks is more complicated, since deposition and cooling may partially overlap and hence a remanence component may be acquired at the same time as the fabric. Moreover, the transportation and deposition dynamics can be highly variable, ranging from concentrated and laminar flows, which form large volume, welded pyroclastic deposits, to highly diluted and energetic turbulent currents, which form surge deposits. However, the reliability of the palaeomagnetic records and the relation between magnetic fabric and emplacement processes was studied earlier (Hillhouse and Wells, 1991; Palmer et al., 1996; Zanella et al., 1999). Furthermore, in pyroclastic deposits, the AMS can be used to determine source vents (e.g. Ellwood, 1982; Urrutia-Fucugauchi, 1983; Baer et al., 1997; Palmer and MacDonald, 1999; Zanella et al., 2001; Wang et al., 2001; Bascou et al., 2005; Alva-Valdivia et al., 2005).

4.2. Results

4.2.1. Lithofacies analysis

Here, a new classification scheme for lithofacies analysis is introduced, combining characteristics of fluvial, mass flow and pyroclastic deposits and integrating them into one comprehensive lithofacies classification system to emphasize the variety and complexity of transport and depositional processes within a volcaniclastic complex. The sediments of the Tepoztlán Formation are dominated by tuffs, tuffaceous breccias, tuffaceous sandstones and conglomerates, and tuffaceous silt- and claystones (see Chapter 2). For the purpose of this study these rocks had been classified into various lithofacies. Based on grain sizes, sedimentary structures, texture, grading patterns and sorting (Tab. 4) a quantitative system for quick and complete field classification was developed. In this study, the classification system yielded 44 different lithofacies types (Tab. 5). The lithofacies code consists of five letters or numbers. A capital letter designating the dominant grain size is followed by one lower case letter which refers to the principal sedimentary structure. The next letter or number describes the texture or the clast to matrix ratio of the lithofacies type. The last two lower case letters refer to grading and sorting characteristics. The lithofacies code *Smxnl* thus refers to the description *Sand, massive, matrix-supported, no grading, very well sorted*. The attributes of the lithofacies types correspond to the stratigraphic mesoscale (Aigner, 1998), giving information on depositional dynamics such as flow velocity etc. Lithofacies codes were used in a purely descriptive sense for recording lithofacies properties. The clastic material (matrix and components) is almost exclusively of volcanic (pyroclastic and autoclastic) origin, independent of the depositional process involved, whether it is primary deposition or after a secondary, fluvial reworking. In this way, non-genetic terms (fines, sand, gravel, etc.) are used to describe grain sizes. The lithofacies types serve as a basis for the interpretation of depositional processes.

Table 4: Lithofacies types with recommended abbreviations and their descriptions.

Recommended abbreviations			
Code position		***Main grain size***	
	D		**D**ust (< 0.002 mm)
	F		**F**ines (silt/ clay) (< 0.06 mm)
1.	S		**S**and (0.06 - 2 mm)
	P		**P**ebbles (2 - 63 mm)
	C		**C**obbles (63 – 200 mm)
	B		**B**oulders (> 200 mm)
		Sedimentary structure	
		m	massive (no bedding)
		l	laminated bedding
2.		h	horizontal bedding
		p	planar cross-bedding
		a	low-angle cross-bedding
		t	trough cross-bedding
		r	ripples
		Texture	
		o	open framework
		s	clast-supported
3.		x	matrix-supported (no clasts)
		3	3 % clasts
		5	5 % clasts
		10	10 % clasts
		15	15 % clasts
		30	30 % clasts
		45	45 % clasts
		Grading	
		n	no grading
4.		g	normal grading
		i	inverse grading
		Sorting	
		v	very poorly sorted
		p	poorly sorted
5.		m	moderately sorted
		w	well sorted
		l	very well sorted

Table 5: Summary of the principal volcanic and sedimentary lithofacies types of the Tepoztlán Formation.

Code	Lithofacies	Remarks	Interpretation	Origin
Fmxgl; Fmxgw	Fines, massive, matrix-supported, normal grading, very well – well sorted	4 cm mean thickness (min. 1 cm, max. 10 cm) predominantly vitric shards. beds uniformly drape the landscape with constant thicknesses.	deposition from a co-ignimbrite ash cloud or phoenix cloud of a pyroclastic density current	P
Flxnw	Fines, laminated bedding, matrix-supported, no grading, well sorted	30 cm mean thickness (min. 10 cm, max. 50 cm) comprises predominantly vitric shards	surge-like depositional conditions from dilute gravity currents or during windy conditions (Allen et al., 1999).	P
Flxgw, Flxgm	Fines, laminate, matrix-supported, normal grading, well – moderately sorted	8 cm mean thickness (min. 5 cm, max. 11 cm)	suspension settling deposition in lacustrine settings or from waning floods. The dark purple colour can be due to pedogenic processes (Jo et al., 1997).	E
Ftxgm	Fines, trough cross-bedding, matrix-supported, normal grading, moderately sorted	20 cm mean thickness	sinuously crested and linguoid (3-D) dunes within fluvial channels (Miall, 1977; Harms et al., 1982; Siegenthaler and Huggenberger, 1993).	E
Frxgl	Fines, ripple cross-lamination, matrix-supported, normal grading, very well sorted	10 cm mean thickness	deposition from waning floods or abandoned channels.	E
Smxnl	Sand, massive, matrix-supported, no grading, very well sorted	5 cm mean thickness comprises crystals and micro-pumice beds uniformly drape the landscape with constant thicknesses.	sustained pyroclastic fall deposition from an eruption cloud	P
Sm15np, Sm15nv	Sand, massive, 15% clasts in matrix, no grading, poorly – very poorly sorted	30 cm mean thickness (min. 10 cm, max. 50 cm)	deposition from a hyperconcentrated flow in a transitional regime between laminar and turbulent flow (Baas and Best, 2002; van Maren, 2007).	E
Smxgl, Smxgw	Sand, massive, matrix-supported, normal grading, very well - well sorted	10 cm mean thickness (min. 5 cm, max. 30 cm) - comprises crystals and micro-pumice - beds uniformly drape the landscape with constant thicknesses.	pyroclastic fall with deposition from an eruption cloud with waning eruption intensity.	P

Code	Lithofacies	Remarks	Interpretation	Origin
Sm3gw, Sm3gp, Sm3gm, Sm5gm, Sm5gp, Sm10gp, Sm15gp	Sand, massive, 3 – 15% clasts in matrix, normal grading, well – poorly sorted	170 cm mean thickness (min. 10 cm, max. 900 cm) possible occurrence of gas escape pipes	deposition from the body and the tail of a pyroclastic flow (Wilson and Walker, 1982), formed by temporal aggradation of material from the dense basal zone of a pyroclastic flow (Branney and Kokelaar, 2002).	P
Sm5ip	Sand, massive, 5% clasts in matrix, inverse grading, poorly sorted	80 cm mean thickness (min. 10 cm, max. 150 cm)	the early stages of deposition from the body of a pyroclastic flow, formed by waxing of flow energy and subsequent transport of coarser lithic clasts further away from the vent (Branney and Kokelaar, 2002) or changes in the supply of coarse lithic clasts from the vent (Pittari et al., 2006).	P
Sm30ip	Sand, massive, 30% clasts in matrix, inverse grading, poorly sorted	140 cm mean thickness (min. 5 cm, max. 280 cm)	hyperconcentrated flow deposits or gradation into massive pumice concentration zones at the top of deposits of pyroclastic flow origin due to waning flow energy and backstepping of the pumice-rich deposit front (Branney and Kokelaar, 2002).	P+E
Shxgw, Shxgm	Sand, horizontal bedding, matrix-supported, normal grading, well – moderately sorted	25 cm mean thickness (min. 5 cm, max. 80 cm)	calm suspension settling deposition in lacustrine settings or deposition in upper flow regime conditions as Upper plane bed sediments (sheet floods)	E
Sh30gm, Sh45gp	Sand, horizontal bedding, 30 – 45% clasts in matrix, normal grading, moderately – poorly sorted	20 cm mean thickness (min. 15 cm, max. 30 cm)	calm suspension settling deposition in lacustrine settings.	E
Saxip	Sand, horizontal bedding, matrix-supported, inverse grading, poorly sorted	50 cm mean thickness	Deposition in upper flow regime conditions as Upper plane bed sediments (sheet floods)	E

Code	Lithofacies	Remarks	Interpretation	Origin
Spxgw, Spxgm, Spxgp	Sand, planar cross-bedding, matrix-supported, normal grading, well – poorly sorted	30 cm mean thickness (min. 10 cm, max. 80 cm)	transverse and linguoid (2-D) dunes within channels or on the top of scours	E
Saxgw, Saxgm	Sand, low-angle cross-bedding, matrix-supported, normal grading, well – moderately sorted		migration of low-relief bedforms	E
Stxnl, Stxnw, Stxnm	Sand, trough cross-bedding, matrix-supported, no grading, very well – moderately sorted	20 cm mean thickness (min. 5 cm, max. 37 cm) comprising crystals and vitric shards local antidunes	pyroclastic surge	P
Stxgl, Stxgw, Stxgm, Stxgp	Sand, trough cross-bedding, matrix-supported, normal grading, very well – poorly sorted	50 cm mean thickness (min. 2 cm, max. 300 cm)	sinuously crested and linguoid (3-D) dunes within fluvial channels or pyroclastic surges	P+E
St15gp, St30gp	Sand, trough cross-bedding, 15 – 30% clasts in matrix, normal grading, poorly sorted	55 cm mean thickness (min. 30 cm, max. 90 cm)	sinuously crested and linguoid (3-D) dunes within fluvial channels	E
Stxiw, Stxim	Sand, trough cross-bedding, matrix-supported, inverse grading, well – moderately sorted	70 cm mean thickness (min. 40 cm, max. 90 cm)	sinuously crested and linguoid (3-D) dunes within fluvial channels or scour-fills	E
St30ip	Sand, trough cross-bedding, 30% clasts in matrix, inverse grading, poorly sorted	100 cm mean thickness (min. 50 cm, max. 160 cm)	sinuously crested and linguoid (3-D) dunes within fluvial channels or in scour-fills	E
Pm45np, Pm45nv	Pebbles, massive, 45% clasts in matrix, no grading, poorly – very poorly sorted	220 cm mean thickness (min. 10 cm, max. 700 cm)	hyperconcentrated flows	E
Pm45gm, Pm45gp	Pebbles, massive, 45% clasts in matrix, normal grading, moderately - poorly sorted	40 cm mean thickness (min. 10 cm, max. 52 cm)	migrating gravel bars with well developed slipfaces	E
Pm30ip, Pm45ip	Pebbles, massive, 30 - 45% clasts in matrix, inverse grading, poorly sorted	10 cm mean thickness	Gradation into massive pumice concentration zones at the top of deposits of pyroclastic flow origin during waning flow energy and backstepping of the pumice-rich deposit front (Branney and Kokelaar, 2002).	P

Code	Lithofacies	Remarks	Interpretation	Origin
Phsgw, Phsgm, Phsgp	Pebbles, horizontal bedding, clast-supported, normal grading, well - poorly sorted	25 cm mean thickness (min. 10 cm, max. 60cm)	calm suspension settling of water-saturated pumice clasts in lacustrine settings or sheet or longitudinal bars or diffuse gravel sheets during waning flow conditions.	E
Ph30gp, Ph45gp	Pebbles, horizontal bedding, 30 – 45% clasts in matrix, normal grading, poorly sorted	35 cm mean thickness (min. 23 cm, max. 80 cm)	sheet floods or diffuse gravel sheets.	E
Phsim	Pebbles, horizontal bedding, clast-supported, inverse grading, moderately sorted	120 cm mean thickness	sheet or longitudinal bars or diffuse gravel sheets during waxing flow conditions.	E
Ppsgm, Ppsgp	Pebbles, planar cross-bedding, clast-supported, normal grading, moderately – poorly sorted	90 cm mean thickness (min. 20 cm, max. 600 cm)	gravel bars or filling of minor channels	E
Pp45gp	Pebbles, planar cross-bedding, 45% clasts in matrix, normal grading, poorly sorted	110 cm mean thickness (min. 20 cm, max. 600 cm)	gravel bar deposits formed by waning flow conditions	E
Ppsip	Pebbles, planar cross-bedding, clast-supported, inverse grading, poorly sorted	160 cm mean thickness (min. 18 cm, max. 650 cm)	gravel bar deposits of longitudinal bars	E
Pp30ip, Pp45ip	Pebbles, planar cross-bedding, 30 – 45% clasts in matrix, inverse grading, poorly sorted	80 cm mean thickness (min. 20 cm, max. 200 cm)	gravel bars or filling of minor channels	E
Ptsgm, Ptsgp	Pebbles, trough cross-bedding, clast-supported, normal grading, moderately – poorly sorted	40 cm mean thickness (min. 10 cm, max. 200 cm)	filling of minor channels or scours or gravely longitudinal bars with well-developed slipfaces formed by waning flow conditions.	E
Pt30gp, Pt45gp	Pebbles, trough cross-bedding, 30 – 45% clasts in matrix, normal grading, poorly sorted	60 cm mean thickness (min. 10 cm, max. 310 cm)	filling of minor channels and scours or gravely longitudinal bars with well-developed slipfaces formed by waning flow conditions.	E
Cmsnp	Cobbles, massive, clast-supported, no grading, poorly sorted	20.0 cm	Lag deposits	E
Cm30nv, Cm30np, Cm45nv, Cm45np	Cobbles, massive, 30 – 45 % clasts in matrix, no grading, very poorly – poorly sorted	315 cm mean thickness (min. 10 cm, max. 1400 cm)	Deposition from visco-plastic debris flows (Shultz, 1984; Costa, 1988)	E

Code	Lithofacies	Remarks	Interpretation	Origin
Cpsgp	Cobbles, planar cross-bedding, clast-supported, normal grading, poorly sorted	130 cm mean thickness (min. 30 cm, max. 300 cm)	gravel bar deposits of longitudinal bars with well-developed slipfaces formed by waning flow conditions	E
Cpsip	Cobbles, planar cross-bedding, clast-supported, inverse grading, poorly sorted	300 cm mean thickness	gravel bar deposits of longitudinal bars with well-developed slipfaces formed by waxing flow conditions	E
Cp45ip	Cobbles, planar cross-bedding, 45% clasts in matrix, inverse grading, poorly sorted	110 cm mean thickness	gravel bar deposits of longitudinal bars with well-developed slipfaces formed by waxing flow conditions	E
Cp30gp, Cp45gp	Cobbles, planar cross-bedding, 30 – 45% clasts in matrix, normal grading, poorly sorted	150 cm mean thickness (min. 40 cm, max. 380 cm)	gravel bar deposits of longitudinal bars with well-developed slipfaces formed by waning flow conditions	E
Ct45gp	Cobbles, trough cross-bedding, 45% clasts in matrix, normal grading, poorly sorted	30 cm mean thickness	scour filling	E
Bm30np, Bm45np	Boulders, massive, 30 – 45% clasts in matrix, no grading, poorly sorted	75 cm mean thickness (min. 20 cm, max. 250 cm)	block-and-ash-flow deposits	P
Bmsgp	Boulders, massive, clast-supported, normal grading, poorly sorted	25 cm mean thickness	scour filling or lag deposits.	E
Bp30gp, Bp45gp	Boulders, planar cross-bedding, 30 – 45% clasts in matrix, normal grading, poorly sorted	85 cm mean thickness (min. 40 cm, max. 150 cm)	gravel bar deposits of longitudinal bars with well-developed slipfaces formed by waning flow conditions	E
Bpsgp	Boulders, planar cross-bedding, clast-supported, normal grading, poorly sorted	60 cm mean thickness (min. 50 cm, max. 70 cm)	gravel bar deposits of longitudinal bars with well-developed slipfaces formed by waning flow conditions	E

Origin: P = pyroclastic; E = epiclastic

4.2.2. Depositional elements

The lithofacies types can be grouped together to form depositional elements (Fig. 9). Based on lithology, external and internal geometries and bounding surfaces, 12 different depositional elements were identified in the field (Tab. 6). Generally, the nomenclature of Miall (1985, 1996) was used for the fluvial and lacustrine deposits; volcanic nomenclature is taken from Fisher and Schmincke (1984), whereas the subdivision into syn-eruptive and inter-eruptive deposits is derived from Smith (1991).

Table 6: Compilation of the 12 depositional elements, together with their depositional processes and eruptive context.

<table>
<tr><th colspan="4">Processes</th><th colspan="2">Depositional elements</th></tr>
<tr><td rowspan="6">syn-eruptive</td><td rowspan="4">primary volcanic</td><td>effusive volcanism</td><td>gravity driven</td><td>LF</td><td>Lava</td></tr>
<tr><td rowspan="3">explosive volcanism</td><td rowspan="3">gas driven</td><td>FA</td><td>Pyroclastic fall</td></tr>
<tr><td>SU</td><td>Pyroclastic surge</td></tr>
<tr><td>PF</td><td>Pyroclastic flow</td></tr>
<tr><td colspan="2" rowspan="2">secondary volcanic</td><td rowspan="6">water driven</td><td>BA</td><td>Block-and-ash flow</td></tr>
<tr><td>DF</td><td>Debris flow</td></tr>
<tr><td rowspan="5">inter-eruptive</td><td colspan="2" rowspan="3">fluvial</td><td>HF</td><td>Hyperconcentrated flow</td></tr>
<tr><td>SF</td><td>Sheet flood</td></tr>
<tr><td>SC</td><td>Scour pool-fill</td></tr>
<tr><td>GB</td><td>Gravel bar</td></tr>
<tr><td>CH</td><td>Channel-fill</td></tr>
<tr><td colspan="2">lacustrine</td><td>LC</td><td>Lacustrine</td></tr>
</table>

Syn-eruptive deposits

Primary volcanic deposits

LF – Lava Flow

The 15 – 25 m thick intermediate massive and brecciated flows characterizing the lava flow elements have an irregular, unconformable contact to the underlying elements. They exhibit a dense core and a vesiculated, rubbly carapace identifying them as a'a flows. Angular fragments of the carapace range from 3 – 50 cm in size at the base or the top of massive flows. The dense core can show columnar jointing. The LF elements are interpreted as viscous, slow moving blocky flows (MacDonald, 1972; Mueller, 1991) as they are associated with lava domes and coulées.

FA – Pyroclastic Fall

Pyroclastic fall elements are composed of phenocrysts and micropumice particles of the same grain size. The elements can show fining-upward as well as coarsening-upward patterns, suggesting waning or waxing eruption intensity, respectively. Thicknesses range from 5 to 10 cm with an average of 5.8 cm. The deposits show mantle bedding disregarding palaeotopography and same thicknesses over wide areas.

Lithofacies types: The element consists of a single lithofacies type which is exchangeable and can be Fmxgl, Fmxgw, Smxnl, Smxgl or Smxgw.

SU – Pyroclastic Surge

Pyroclastic surge elements mainly consist of glass shards, phenocrysts and subordinate pumice particles of ash to lapilli size. The dominating grading pattern is fining-upward, suggesting waning flow energies. The elements are characterised by migrating dunes, in some cases antidunes, showing transitions between upper and lower flow regime. Thicknesses range from 5 to 10 cm with an average of 7.5 cm. The deposits show pinch-and-swell structures. The lower surfaces can be flat, although local erosional surfaces can be recognized. Their top is frequently erosive.

Lithofacies types: The element consists of a single lithofacies type which is exchangeable and can be Flxnw, Stxnl, Stxnw, Stxnm, Stxgl, Stxgw, Stxgm or Stxgp.

PF – Pyroclastic Flow

Pyroclastic flow elements are crystal- and pumice-rich, mainly consisting of accessory and minor cognate lithic fragments in a matrix of bubble wall shards and phenocrysts. They are generally non-welded, however, incipient welding was recognized. The elements usually show a normal coarse-tail grading of the lithic clasts while the pumice clasts show a reverse grading. Thicknesses of single flow units can vary from 0.1 to 9.0 m with an average of 1.5 m. The deposits are partly draping the pre-eruption topography, thickening in valleys and depressions. Their lower bounding surfaces are flat or reflecting the palaeosurface, their tops are mostly erosive. The elements occur as single units or as a series of stacked beds.

Lithofacies types: Relatively thin PF elements can consist of only one lithofacies type (Sm3gw, Sm3gp, Sm3gm, Sm5gm, Sm5gp, Sm10gp, Sm15gp). The same types can form the body of thicker PF elements, depending on their content in coarse clasts. The lithic-rich base of thicker PF elements is characterised by the lithofacies type Sm5ip while the pumice-rich top is indicated by Sm30ip, Pm30ip or Pm45ip, depending on the pumice content.

BA – Block-and-ash Flow

The block-and-ash flow elements are characterised by matrix-supported, poorly sorted monomict tuff breccias with flat or erosive bases and flat upper surfaces. Thicknesses vary from 1.1 to 2.7 m with an average of 1.8 m. The deposits pinch out laterally and consist of angular, sometimes hexagonal, nonvesiculated dacitic to andesitic clasts in a fine-grained matrix of the same chemical composition. Pumice clasts as well as welding features are absent. These massive boulder-rich elements are interpreted to be derived from small-volume pyroclastic flows, generated by explosive disruption or the sudden gravitational collapse of a lava dome. Coarse grain-sizes and the lack of associated lava flows suggests proximal to medial deposition.

Lithofacies types: The element consists of a single lithofacies type which is exchangeable and can be Bm30np or Bm45np.

Secondary volcanic deposits

DF – Debris Flow

Debris flow elements appear interbedded between gravel and pyroclastic deposits. They occur in lateral extensive (up to several 100 meters) sheets with planar bases and erosive tops. Average thicknesses of single elements are about 4 m, however, vertical amalgamation surfaces are rarely visible for which reason up to 14 m thick debris flow deposits were found without any visible bounding surfaces. The elements are characterised by matrix-supported diamictons that may be associated laterally and vertically with sand-dominated heteroliths. The pebble- to cobble-sized clasts are clearly of the same origin as block-and-ash flow and pyroclastic flow deposits, recognized in a matrix of reworked ash. The composition of the DF elements suggests a deposition from lahars in the proximity of a stratovolcano.

Lithofacies types: The element consists of a single lithofacies type which is exchangeable and can be Cm30nv, Cm30np, Cm45nv or Cm45np.

HF – Hyperconcentrated Flow

The sand-dominated hyperconcentrated flow elements are associated laterally and vertically with DF elements. Both are similar in extension as well as in the appearance of their bounding surfaces, showing lateral extensive sheets with extensions up to several 100 m and often planar surfaces. Locally, basal surfaces show erosional (then concave-up) bases and erosive tops. Thicknesses vary between 0.1 and 6 m, although stacked units up to 28 m without clearly visible bounding surfaces can appear. Composition of these elements is the same as in associated DF elements pointing to an origin from lahars. They mark the distal part of the lahar in transition from laminar to dilute flow.

Lithofacies types: The element consists of a single lithofacies type which is exchangeable and can be Sm15np, Sm15nv, Sm30ip, Pm45np or Pm45nv.

Inter-eruptive deposits

Fluvial deposits

SF – Sheet Flood

The relatively thin, sandy sheet flood elements are locally preserved within the gravel deposits. They have flat, erosive bases and an erosive upper bounding surface. Laterally, individual elements pinch out or are eroded and extend more than 150 m. Thicknesses vary from 0.1 to 0.8 m with an average of 0.2 m. These elements are interpreted as upper-stage plane bed deposits. Their preservation potential within a gravel-bed river is relatively low (Kostic et al., 2007).

Lithofacies types: The element consists of a single lithofacies type which is exchangeable and can be Shxgw, Shxgm, Saxip, Phsgw, Phsgm, Phsgp, Ph30gp, Ph45gp or Phsim.

SC – Scour pool-fill

The shape of these elements is characterised by an erosive concave-up lower bounding surface. If the upper surface is erosive, an interaction with other elements is observed. The internal structure consists of trough cross-bedded gravels and sand. Thicknesses can range

from 0.1 to 6 m with an average of 0.8 m. These elements are interpreted to represent scour pool fills formed within channels as they are most common within braided rivers.

Lithofacies types: The basis of cut-and-fill structures are mostly characterised by very coarse deposits (Ct45gp or Bmsgp) and then a multi-phase filling and coarsening upward from gravels (Ptsgm, Ptsgp, Pt30gp or Pt45gp) to sandy sediments (Stxiw or Stxim). Rarely, an inverse grading can be seen within the sands (St30ip). The top of the scour-fills is mostly characterised my planar cross-bedded sands (Spxgw, Spxgm or Spxgp).

GB – Gravel Bar

The gravel bar elements show flat upper and lower bounding surfaces, pinching out laterally. Lower surfaces tend to be erosive. The cross-bedded elements are mostly composed of pebble- or cobble-rich, more rarely by boulder-rich gravel. They form single beds or sets of stacked beds. Thicknesses vary from 0.2 to 6 m with an average of 1 m.

Lithofacies types: The gravel bar elements usually show a fining-upward from boulder- (Bp30gp, Bp45gp, Bpsgp) or cobble-rich (Cpsgp, Cpsip, Cp45ip, Cp30gp, Cp45gp) to pebbly material (Pm45gm, Pm45gp, Ppsgm, Ppsgp, Pp45gp, Ppsip, Pp30ip, Pp45ip, Pt30gp, Pt45gp). The lithofacies types are exchangeable and change according to the transport energy or the available material.

CH – Channel-fill

The channel elements consist of tuffaceous sandstones, comprising glassy material from reworked pyroclastic elements as well as small lava and pumice particles and minor rounded phenocrysts, dominated by feldspars and pyroxenes.
Fining-upward successions are common, often with clayey layers on top, pointing to very low flow energies after a relocation of the main channel within the braided stream.
Trough cross-bedding is the dominant sedimentary structure within the channel element. However, planar cross-bedding or ripples are also common. Individual channel fills are stacked, often forming multilateral and single- or multistorey channel belts. The thickness of the CH elements ranges from 0.1 to 3.1 m with an average of 0.4 m. The lateral extend of single channels cannot be determined clearly in all cases; however, some outcrops show extends of up to 150 m. They are characterised by shallow concave-up to flat bases. The upper bounding surfaces are always erosive. Laterally, individual elements pinch out or are completely eroded away.

Lithofacies types: Channel-lag deposits are possible at the base and consist of Cmsnp or Bmsgp. The elements mostly consist of multi-phase fillings of stacked lithofacies types showing a fining-upward. Here, the lithofacies types Ptsgm, Ptsgp, Spxgw, Spxgm, Spxgp, Saxgw, Saxgm, Stxgl, Stxgw, Stxgm, Stxgp, St15gp, St30gp, Stxiw, Stxim or St30ip are exchangeable. In the upper part of the element a high mud content is common due to waning flow conditions (Ftxgm, Frxgl).

Lacustrine deposits

LC – Lacustrine

Lacustrine elements are dominated by sub-cm- to dm-thick laminated claystones. In lakeshore positions they may contain horizontally bedded sand and pumiceous drop stones, derived from subaerial pyroclastic falls. Thicknesses vary from 0.1 to 1 m with an average of 0.5 m.

Lithofacies types: Thin veneers mostly consist of either Flxgw or Flxgm, Thicker deposits, especially near the former lake-shore can show grading-upward from the former clayey-silty sediments to the lithofacies types Shxgw, Shxgm, Sh30gm, Sh45gp, Phsgw, Phsgm and Phsgp. The different sandy and pebbly sediments are exchangeable at a time.

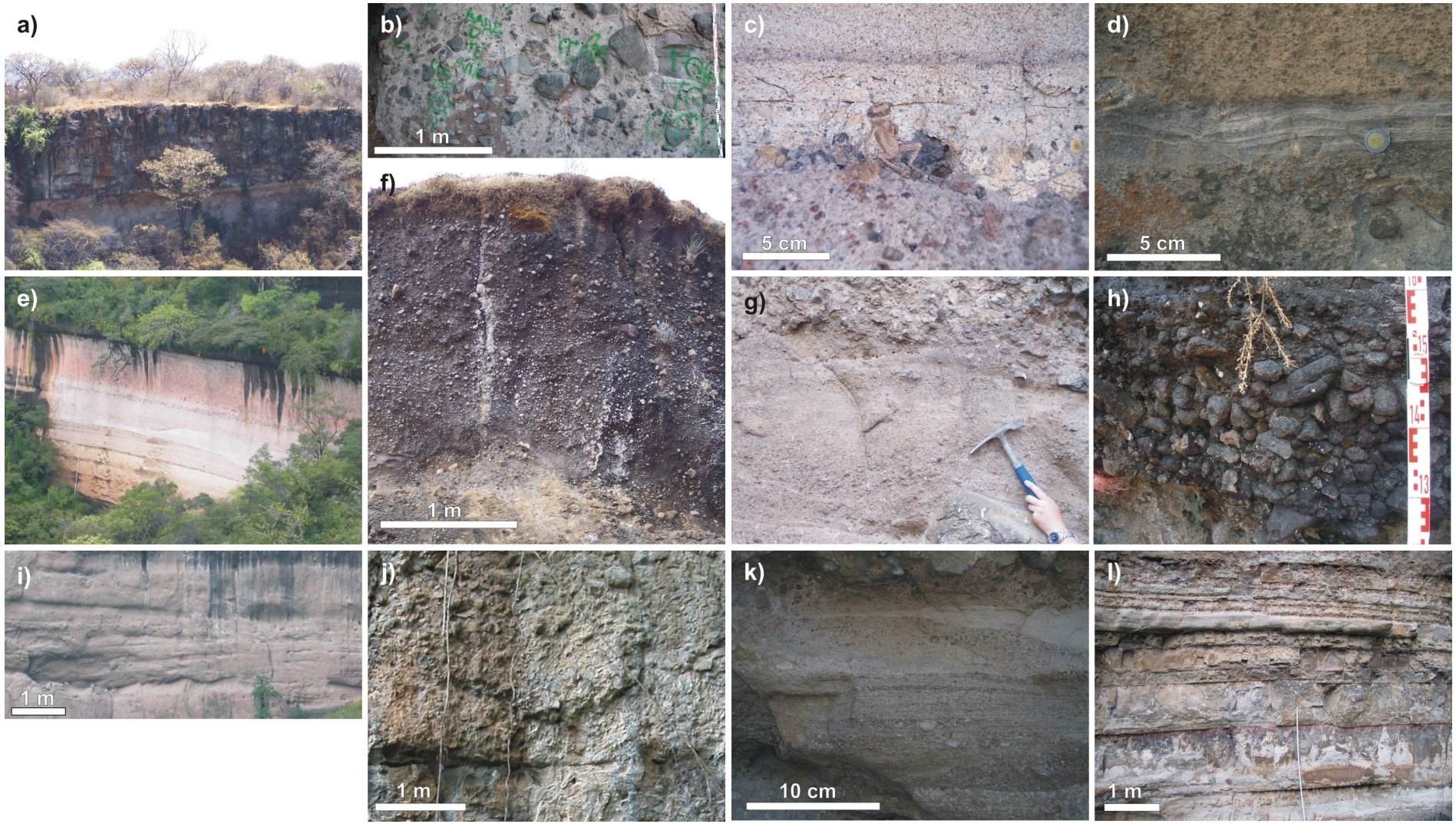

Figure 9. Photographs showing examples of the architectural elements: a) LF (Lava flow), b) FA (Pyroclastic fall), c) SU (Pyroclastic surge), d) PF (Pyroclastic flow), e) BA (Block-and-ash flow), f) DF (Debris flow), g) HF (Hyperconcentrated flow), h) GB (Gravel bar), i) CH (Channel-fill), j) SC (Scour-fill), k) SF (Sheet flood), l) LC (lacustrine).

4.2.3. Depositional architecture

The six analysed locations provide successions of pyroclastic density current, lahar and fluvial deposits along several hundred meters in width and height, respectively. Lithostratigraphic sections are discussed in context with related medium scale panels. If appropriate, descriptions of small scale panels from Trauth (2007) are included to verify interpretations by analyzing the spatial distribution of different lithofacies types within a small scale that can not be described in medium scale panels.

Volcaniclastic deposits in Malinalco

In the east of Malinalco, the Tepoztlán Formation is at least 330 m thick. Three 2D-panels (two medium scale and one large scale panel) and a detailed stratigraphic section were constructed in the Malinalco area (Fig. 5). Here, the volcaniclastic strata of the section and the two medium scale panels range in age from 22.8 to 22.1 Ma, belonging to the Malinalco and San Andrés Members of the Tepoztlán Formation.

Stratigraphic section MA

The Malinalco section (MA) is located southeast of Malinalco (18.93°N, 99.48°W). It attains a thickness of 93 m and can be followed through the medium scale panel 1.1. (Fig. 10). The section is mainly composed of tuffaceous sandstones and tuffs with minor amounts of clay- and siltstones. The dominant facies are channel-fill and gravel bar elements. Gravel bars are increasing to the top and show a coarsening- and thickening-upward trend. Pyroclastic flow deposits are prevalent while pyroclastic surge and fall and lacustrine elements occur only occasionally. Pyroclastic flow elements occur in regular intervals.

Medium scale panel 1.1.

The base of panel 1.1. (Fig. 11) as well as section MA is characterised by the deposition of at least two thick pyroclastic flows, containing vertical hexagonal cooling cracks. There are signs for fluvial reworking and scouring in between. The orientation of the scours shows a NW-SE direction. The top of the stacked pyroclastic flow layers is marked by the deposition of fluvial elements. Furthermore, there is an abundance of overlapping channels, laterally with transitions to gravel bars and scours. These sediments are covered by about 3 m thick sheet-flood deposits before once again predominant overlapping channel elements occur with minor gravel bars. Small, clast-supported lag deposits occur along channel and scour surfaces. Channel-fill elements are dominant for the lower half of the panel. In the upper half the frequency of channel-fill elements decrease and coarse gravel bar elements increase throughout the panel. Throughout stratigraphy, the gravel bar elements become coarser and thicker, showing a coarsening- and thickening-upward trend and are sometimes cut by scours

or minor channel elements. Pyroclastic flow elements occur in regular intervals of 5 to 15 m. Especially in the lower half thin (about 5 cm thick) surge deposits can be found below these elements, sometimes with pyroclastic fall layers on top, predominantly consisting of micropumice. In the upper third of the panel one channel (SSW-NNE orientation) is filled by a pyroclastic flow element, followed by 1 m thick lacustrine sediments. The base of the lacustrine sediments is characterised by clayey to silty layers (1 to 5 cm in thickness) that grade into sandy and gravely layers with a high concentration in pumice particles. To the left (NNW), the thickness of the lacustrine sediments decreases to about 20 cm. Here, the coarsest grain sizes can be found. To the left, the stacked lacustrine sediments are covered by another pyroclastic flow, to the right by a sheet-like debris flow, partly scouring into the pyroclastic flow.

Medium scale panel 1.2.

Panel 1.2. (Fig. 12) is located 150 m SE of panel 1.1. It shows similar sedimentary patterns as the latter. Especially the coarsening- and thickening-upward trend within the panel, due to an increase of thick gravel bars, can be clearly noticed. The lacustrine sediments in the middle of the panel attain a thickness of about 2-3 m and give evidence for the area that was covered by the lake, having a length of at least 430 m. However, unlike the lacustrine sediments in panel 1.1., showing a coarsening-upward up to coarse sand grain sizes, the entire package consists of silt- and claystone. The panels show signs of block faulting. The block containing the lacustrine sediments is tilted with about 15° to the north.

Large scale panel 1.3.

Fig. 13 shows the position of 1.1. and 1.2. within the large scale panel 1.3. The large scale panel shows the entire mountain range which is formed by the Tepoztlán Formation east of Malinalco. Fluvial sedimentation dominates throughout the entire panel, and is only interrupted by the deposition of minor intercalated pyroclastic flows.

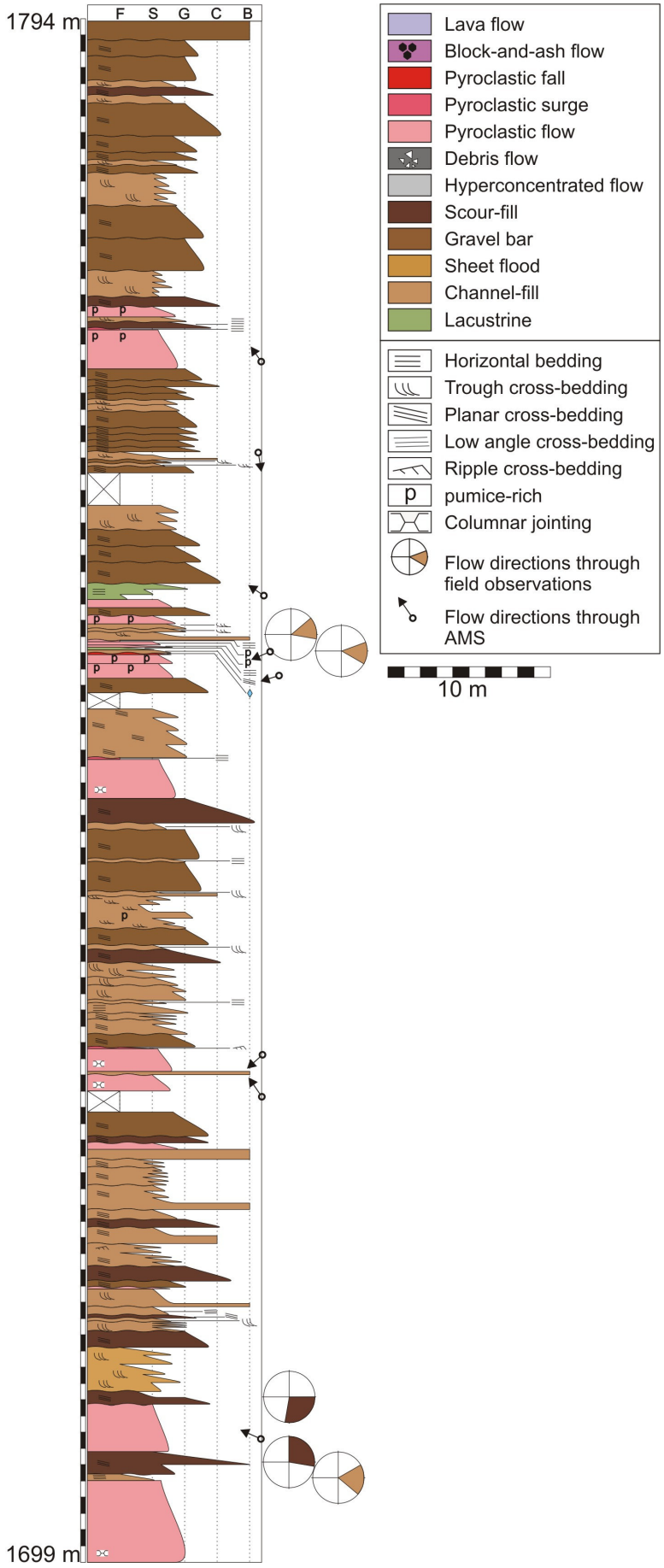

Figure 10. Lithostratigraphic section (MA) of the Tepoztlán Formation near Malinalco.

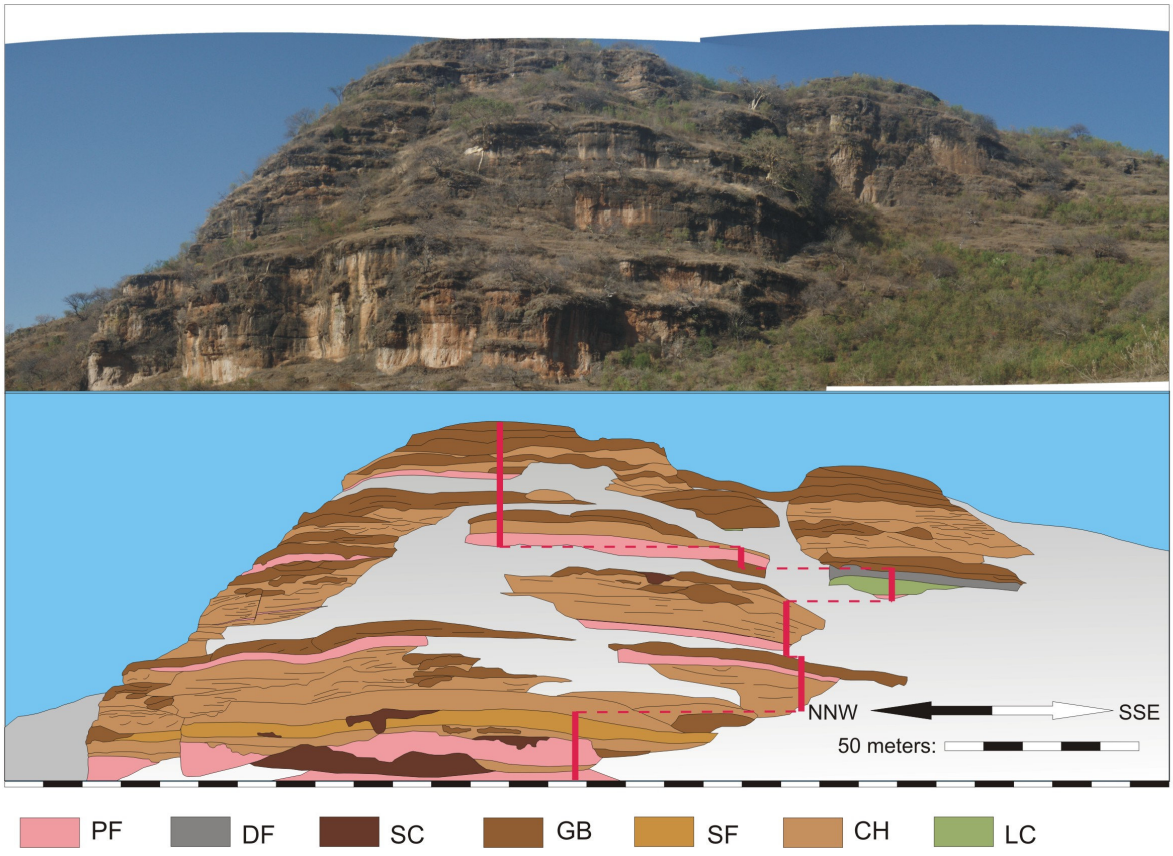

Figure 11. Medium scale panel 1.1. (a) Photomosaic of the study outcrop. (b) Interpretation of the photomosaic. The red line shows the course of the stratigraphic section. PF, pyroclastic flow; DF, debris flow; SC, scour-fill; GB, gravel bar; SF, sheet flood; CH, channel-fill; LC, lacustrine. The red line indicates the course of the stratigraphic section MA.

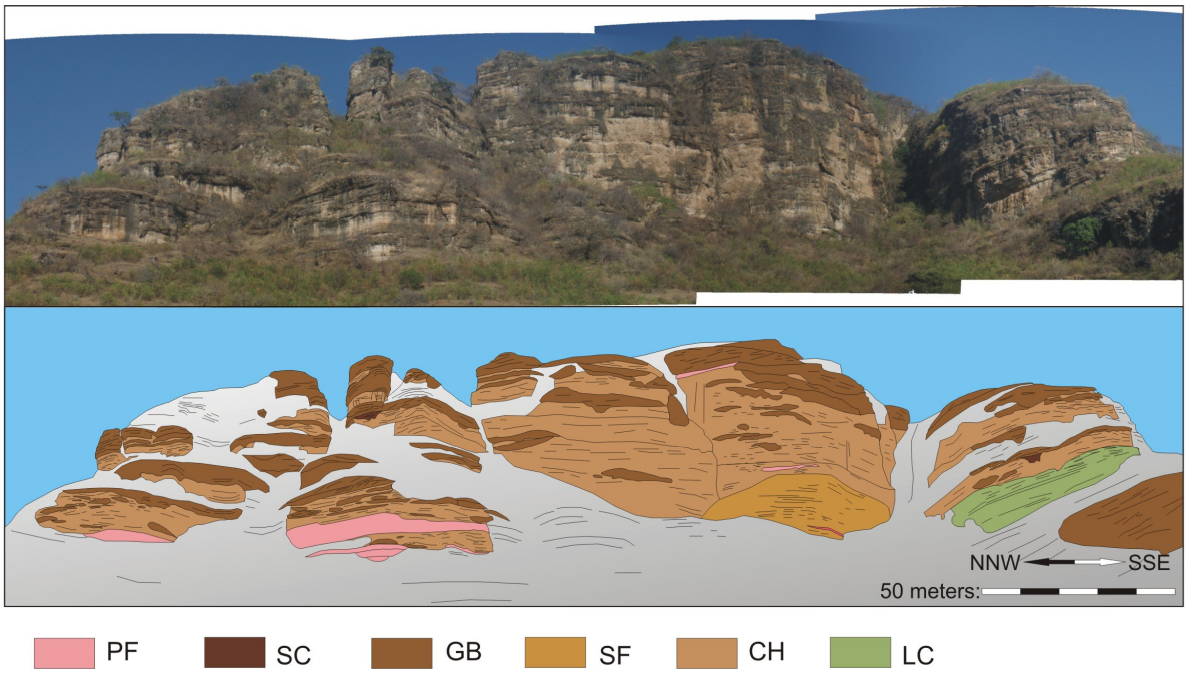

Figure 12. Medium scale panel 1.2. (a) Photomosaic of the study outcrop. (b) Interpretation of the photomosaic. PF, pyroclastic flow; SC, scour-fill; GB, gravel bar; SF, sheet flood; CH, channel-fill; LC, lacustrine.

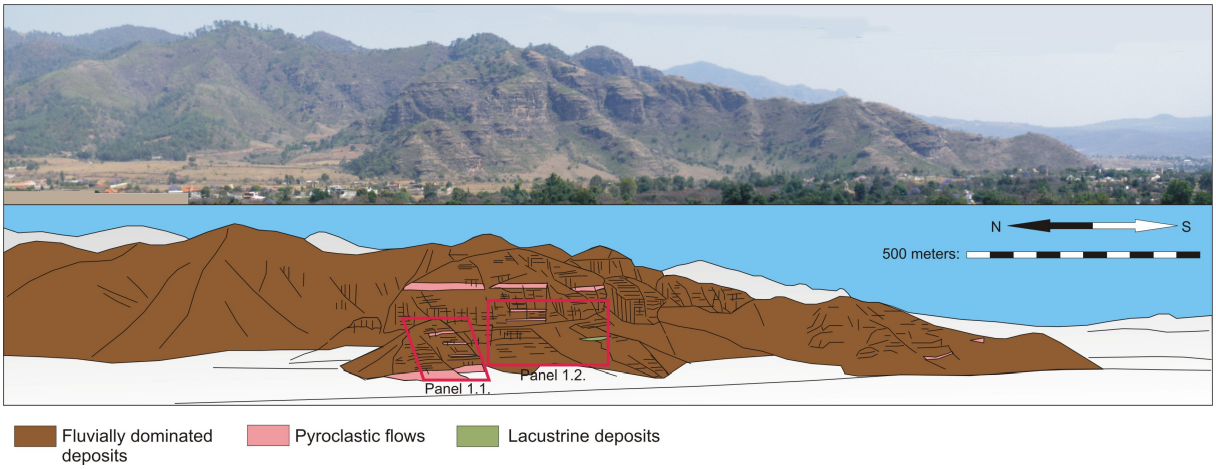

Figure 13. Large scale panel 1.3. (a) Photomosaic of the study outcrop. (b) Interpretation of the photomosaic. The locations of the 2D-panels 1.1. and 1.2. are indicated by the red frames.

Interpretation

In Malinalco the evolution of the Tepoztlán Formation started with a phase of high explosive volcanism, characterised by the deposition of at least two thick (about 5 m) pyroclastic flows at the base of the succession. Signs for scouring by a river and relatively thin fluvial sediments in between indicate that the deposition of the pyroclastic flows took place close to or within a fluvial system that tried to follow its original course during eruptions. The sheet flood deposits on top of these sediments are interpreted to have been formed at the front of a volcanic induced alluvial fan, at the transition to the river system and give evidence for the proximity of the volcanic source.

The next 15 m of the succession are dominated by fluvial sediments, indicating an inter-eruptive period of relative quiescence. However, the explosive volcanic activity had not ceased completely during this time as the occurrence of relatively thin (few 10s of centimetres) pyroclastic flow deposits give evidence. Furthermore, it can be noticed that the clastic material of the fluvial sandstones and conglomerates is of volcanic origin exclusively. This shows that the volcanic activity continues in the hinterland of the study area. However, in times of minimized volcanic activity, pyroclastic flows either do not reach this location anymore or are reworked by the stream immediately after deposition.

Based on the abundance of amalgamated channels and the continuous upward gradation this part is interpreted to represent an initially high-energy braided stream system. The fluvial sediments are dominating all throughout the entire sedimentary succession of the Tepoztlán Formation in this location. There is a noticeable trend of thickening- and coarsening-upward within the succession, characterised by a transition from relatively thin sandy channel-fills to coarser and thicker gravel bars to the top. Deep scours however, mostly occur together with the sandy channel deposits and decrease with the increasing coarse conglomerates of the gravel bars. The thickening- and coarsening-upward trend is interpreted as a deposition in a moderately aggradational setting that is related to a steepening of the relief, caused by the

development of one or more volcanic structures in the near vicinity. However, mass flow deposits are still absent in the entire section except one in its upper part. In regular intervals, the fluvial sedimentation is interrupted by the deposition of a stack of pyroclastic flow deposits. In higher parts of the stratigraphic section and the panels, the deposition of pyroclastic surges and pumice falls, coexisting with the pyroclastic flow elements, is recorded. The regular occurrence of the pyroclastic flow deposits points to explosive volcanic activity in regular time intervals while surge deposits indicate a deposition proximal to the source area. What is particularly of interest in this location is the development of a lake within the volcaniclastic sediments. The stratigraphic section and the two medium scale panels are interpreted to document the deposition of a pyroclastic flow within a fluvial channel that led to the damming of the original river and thus to a backblock of the stream and the development of a lake. The centre of the lake is characterised by mostly clayey to silty sediments in panel 1.2. while panel 1.1. most probably represents the shoreline with a prograding river-delta providing sandy sediment from NNW direction. In panel 1.1. the lacustrine deposition was stopped by another pyroclastic flow which filled the lake basin and which was later partly entrained into the following lahar, characterised by debris flow deposits.

Volcaniclastic deposits in San Andrés

North of the village of San Andrés de la Cal (18.95°N, 99.11°W) the Tepoztlán Formation attains a thickness of about 370 m. Two detailed stratigraphic sections and six 2D-panels (two small scale panels and four large scale panels) were constructed in this area (Fig. 5). The volcaniclastic strata of the stratigraphic sections range in age from 22.8 to 21.3 Ma, belonging to the Malinalco and San Andrés Members of the Tepoztlán Formation.

Stratigraphic sections SA1 and SA2

The San Andrés section 1 (SA1) with a thickness of 183 m is located north of the village San Andrés (Fig. 14). The lower part of the section is dominated by pyroclastic flow deposits, gravel bars and minor debris flow deposits. With increasing altitude more and more pyroclastic flow elements enter the system. On top of a stack of pyroclastic flow deposits several lobes of a block-and-ash flow can be found. The upper pyroclastic flow element contains gas escape pipes. The top of the section is dominated by pyroclastic flow elements and minor amounts of their reworking products in the form of fluvial and debris flow deposits. The San Andrés 2 section (SA2), 100 m east of SA1 attains a thickness of 92 m. The lower and the middle part are almost only composed of pyroclastic flow deposits which can be correlated quite well with the corresponding strata in SA1. The top of this section shows an increase in fluvial deposits.

Small scale panel 2.1.

Representative for the fluvial sediments in the lower part of the succession, the small scale panel 2.1. shows a gravel bar dominated depositional system (see Trauth, 2007; Fig. 15). The gravel bar elements at the base of the panel are characterised by planar cross-bedding and thicknesses between 30 cm and 1.30 m. Following these elements, a 20 to 30 cm thick pyroclastic flow element can be traced over the entire panel. The element is covered and partly scoured by another stack of gravel bars. What is remarkable in this panel is, that a clear normal fault in its left part can be seen, crossing the pyroclastic flow element and the gravel bar on top. Higher gravel bar elements are not affected. The right part of the panel is lowered by about 50 cm. Furthermore, a well rounded block of 2.5 m in diameter can be found next to the fault. The layers below contain bomb sack structures.

Small scale panel 2.2.

Representative for the pyroclastic flow dominated part of the Tepoztlán Formation, panel 2.2. shows a succession of several pyroclastic flow, surge and fall deposits (see Trauth, 2007; Fig. 16). The base of the panel is characterised by a thick pyroclastic flow deposit. Following this element a succession of stacked pyroclastic surges can be noticed, showing signs of erosion in the left and right part of the panel. Especially in the right part, this erosion was caused by the formation of a fluvial channel as there are still remains of sandy channel-fill elements. Chunks of the pyroclastic flow deposit can be traced within the fluvial sediments. The fluvial channel is filled by a stack of three pyroclastic flow elements. Simultaneously, a fall layer can be traced throughout large parts of the panel but was partly eroded by subsequent pyroclastic flows. On top of this stack, a very pumice-rich ignimbrite can be traced over the entire panel, followed by at least two more thick, lithic-rich sheets of ignimbrites.

Large scale panel 2.3.

The large scale panel 2.3. shows a part of the San Andrés Member of the Tepoztlán Formation, dominated by pyroclastic flow elements, with W-E orientation from San Andrés in the south (Fig. 17). The courses of the two stratigraphic sections SA1 and SA2 are indicated by red lines.

Large scale panel 2.4.

The large scale panel 2.4. shows the Tepoztlán Formation with E-W orientation from Tepoztlán in the north (Fig. 18). Its lower part is dominated by fluvial deposits while pyroclastic flow elements become increasingly important with higher elevations. Especially in the western part, the top is dominated by debris flows. The orientation and transport direction of the mass flow dominated system can not be clearly seen in this panel. However, the main transport direction of the mass flow deposits can be documented in the following panel.

Large scale panel 2.5.

Panel 2.5. (Fig. 19) has a N-S orientation, showing the Tepoztlán Formation north of San Andrés and north of Tepoztlán from the west. A dominance of fluvial deposits with occasional pyroclastic flow elements can be noticed in the lower half of the panel while debris flow deposits are dominating in the upper half. The transport direction of the mass flow dominated sediments was from north to south.

Large scale panel 2.6.

A similar picture like panel 2.5. is received from panel 2.6. (Fig. 20) at the eastern side of the mountain range north of San Andrés. This panel has a S-N orientation. While sandy channel elements and gravel bars are dominating in the south, sheet-flood elements are intervening from the north. These are followed by debris flow deposits. However, the debris flow deposits rarely reach the southern edge of the panel. Pyroclastic flow deposits are abundant throughout the panel.

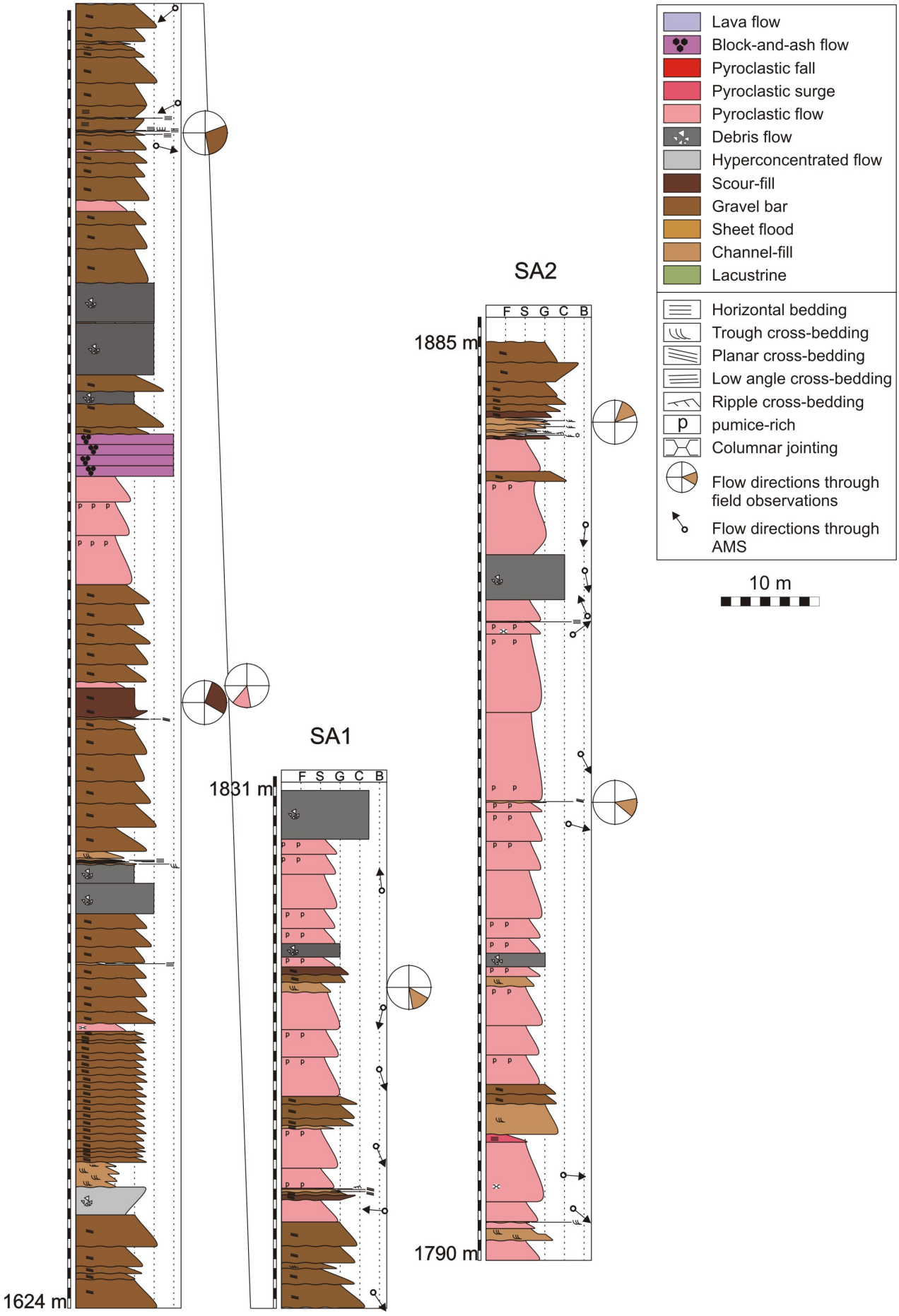

Figure 14. Lithostratigraphic sections SA1 and SA2 of the Tepoztlán Formation near San Andrés.

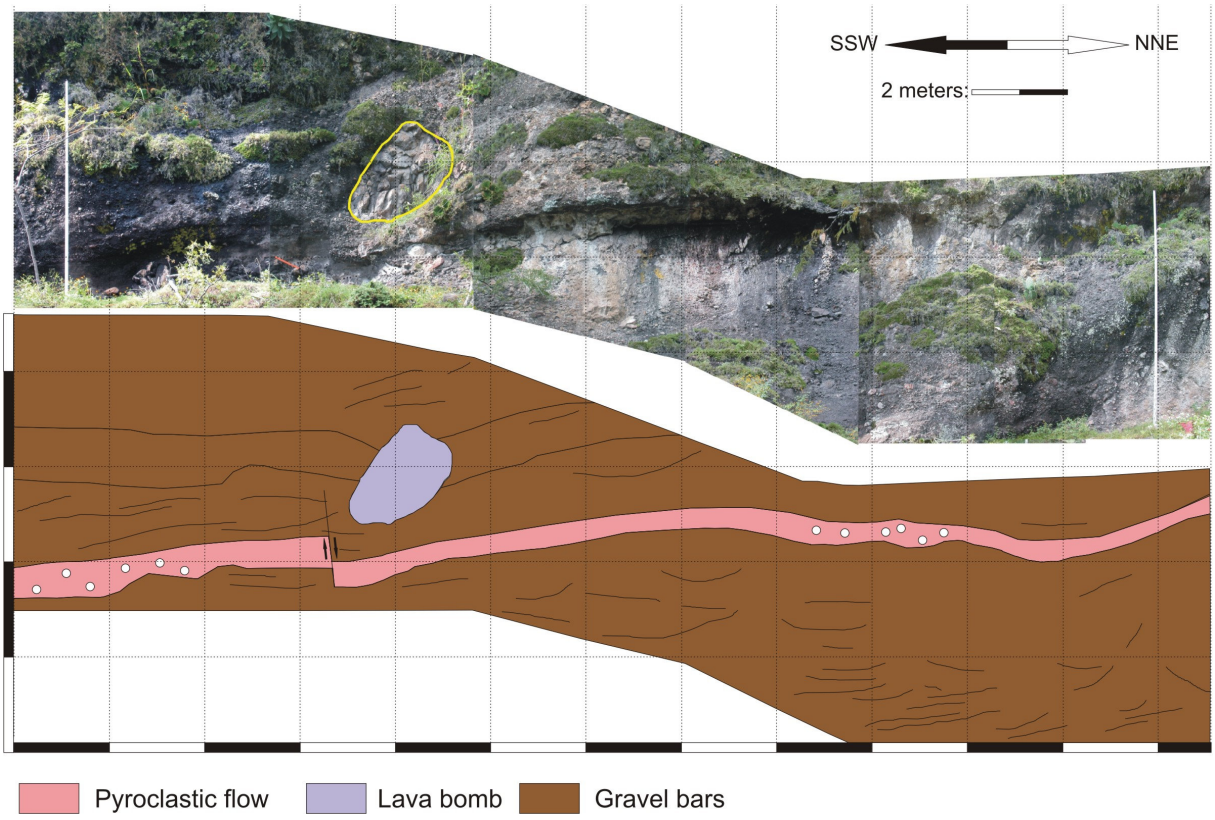

Figure 15. Small scale panel 2.1. (a) Photomosaic of the study outcrop. (b) Interpretation of the photomosaic.

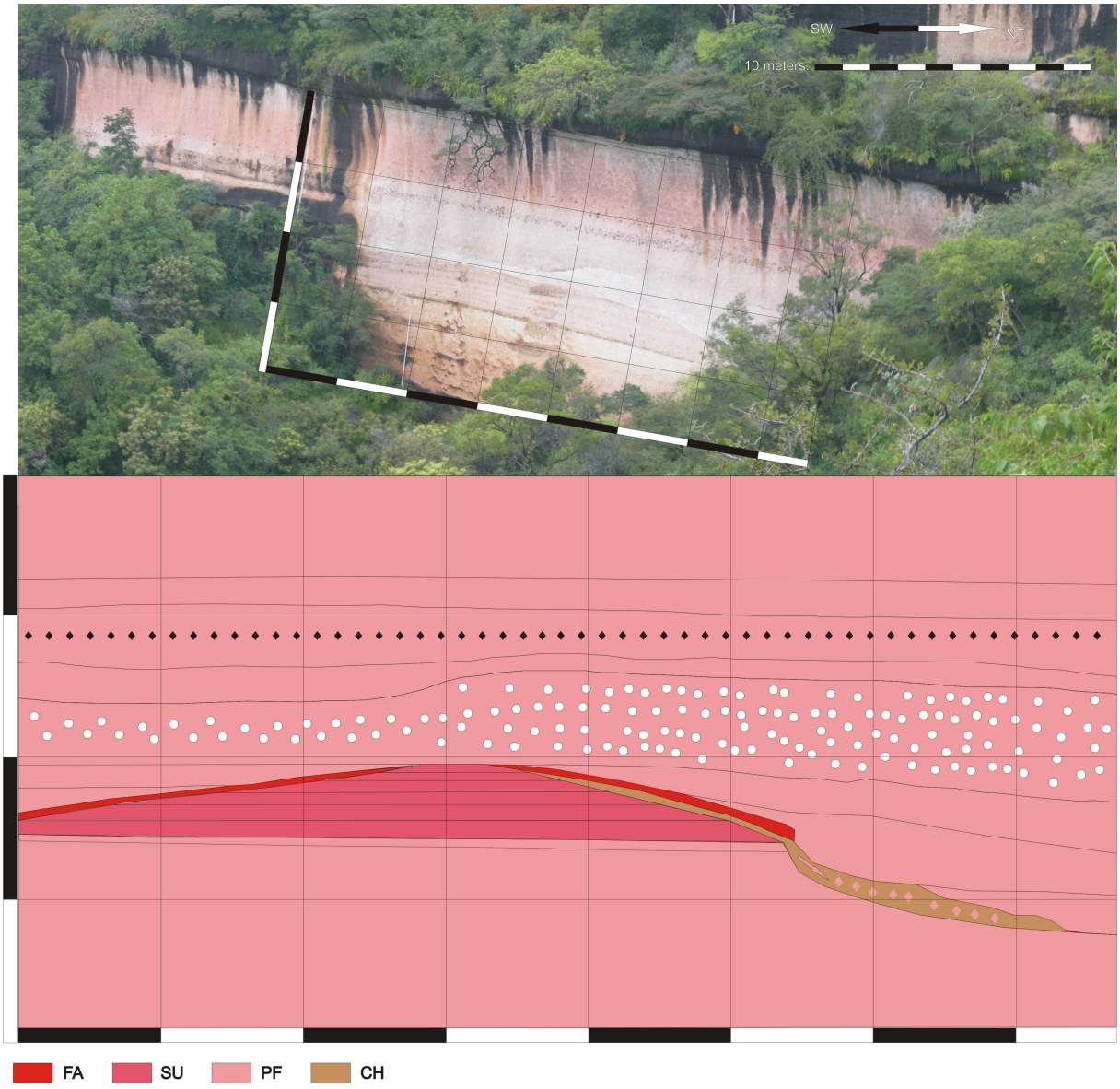

Figure 16. Small scale panel 2.2. (a) Photomosaic of the study outcrop. (b) Interpretation of the photomosaic. FA, pyroclastic fall; SU, pyroclastic surge; PF, pyroclastic flow; CH, channel-fill.

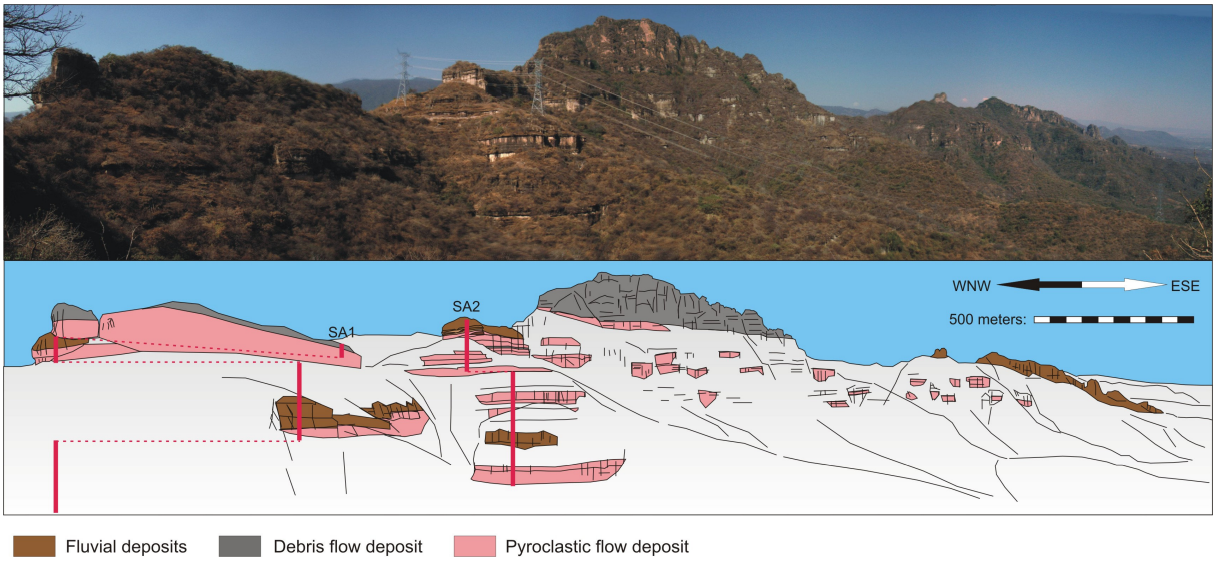

Figure 17. Large scale panel 2.3. (a) Photomosaic of the study outcrop. (b) Interpretation of the photomosaic. The red lines indicate the courses of the sections SA1 and SA2.

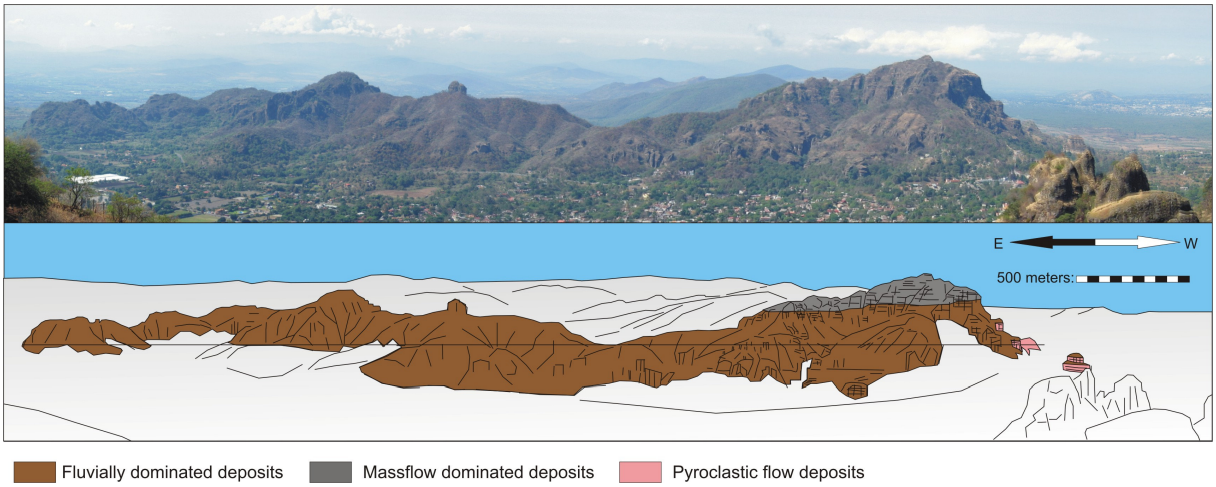

Figure 18. Large scale panel 2.4. (a) Photomosaic of the study outcrop. (b) Interpretation of the photomosaic.

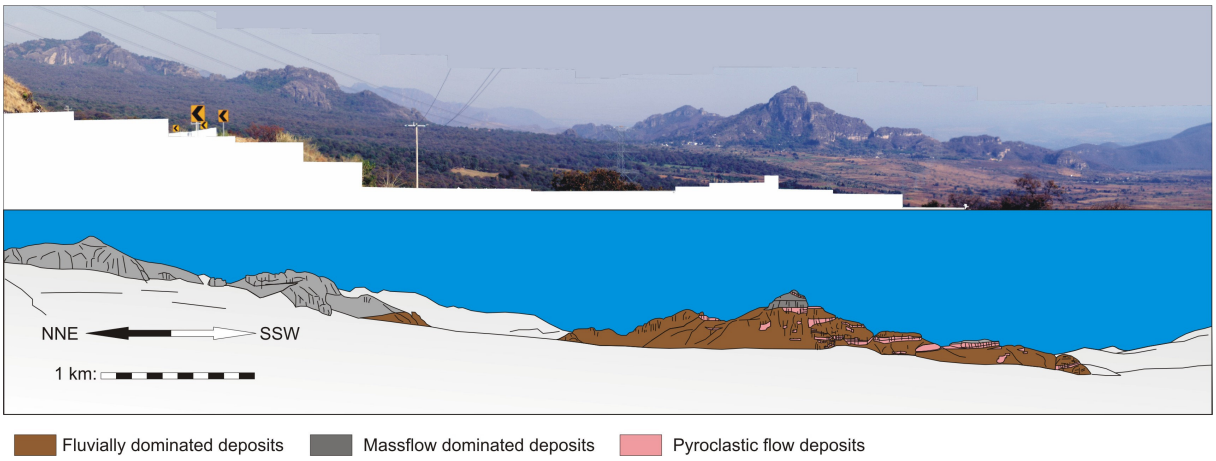

Figure 19. Large scale panel 2.5. (a) Photomosaic of the study outcrop. (b) Interpretation of the photomosaic.

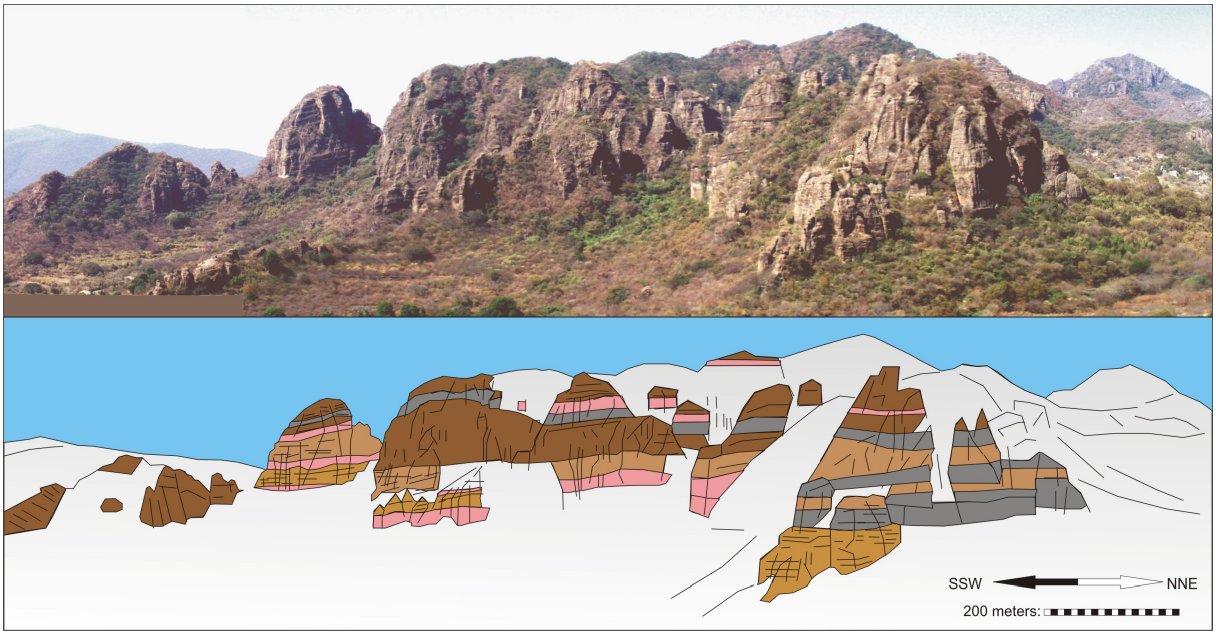

Figure 20. Large scale panel 2.6. (a) Photomosaic of the study outcrop. (b) Interpretation of the photomosaic.

Interpretation

The lower part of the succession, i.e. the oldest exposed deposits of the Tepoztlán Formation within the study area, at the base of section SA 1 is characterised by sandy channel-fills and gravel bars with single intercalated mass flow deposits, ranging from hyperconcentrated flows to debris flows. Orientations of imbricated gravels, scour walls and mapped palaeochannels indicate that a fluvial transport direction from east to west was dominating with a lightly radial dispersal pattern. The predominance of low-angle erosional surfaces, small bouldery gravel bars, and flat-bedded to crossbedded, tuffaceous sand supports deposition in a system of shallow migrating channels with longitudinal bars, diffuse gravel sheets, and unstable banks. Based on the abundance of overlapping channels and the continuous upward gradation this part is interpreted to represent an initially high-energy braided stream system. Small, clast-supported lag deposits occur along channel and scour bases. The pumiceous, sand- to granule-size matrix strongly suggests reworking of unlithified ash. The coarse-grained volcanic debris was probably transported to the area by debris flows, but only remnants can be noticed in the lower part of section SA1. An indication for synsedimentary tectonic activity is the normal fault in 2.1. which probably formed during an earthquake due to volcanic activity. The block next to the fault is interpreted to present a volcanic bomb. By means of the bomb sack structures a flight direction from NNE to SSW can be proposed. The outcrops of bedded, reworked tuff along with the accumulation of debris flow and stream deposits in broad, shallow channels suggest deposition in a moderately aggradational setting of low relief. In the middle part of section SA1 stacked layers of orange to pink, lithic-rich tuff, as thick as 11 m belong to the oldest primary, non-reworked volcaniclastic material and give direct evidence for explosive activity. Vertical gas-escape structures are common in these

deposits. They are covered by several successional layers of blocky tuff breccia, originating from block-and-ash flows. Their deposition was followed by reworking of the provided material within the streambed or due to lahars, causing the deposition of debris flows. Locally, interstratified lava flows, representing near-vent facies, give evidence for effusive eruptions and were the dominant source for the volcanic detritus preserved in the sections.

On top of the lava flows, another about 40 m thick package of amalgamated and stacked gravel deposits is exposed with minor intercalated pyroclastic flow deposits.

The vertical transition from sandy deposits to thicker conglomerates reflects a change in the fluvial architecture. The fluvial patterns are characterised by a coarsening- and thickening-upward trend and thus an increase of incorporated primary volcanic material, pointing to an increasing volcanic intensity in the volcanic source area. This hypothesis is strongly supported by the occurrence of near-vent block-and-ash-flows and abundant ash flow tuffs that are increasingly occurring towards the upper part of the succession, suggesting a progressive progradation of the volcanic system. The tops of section SA1 and section SA2 are clearly dominated by pyroclastic flow deposits, recording a major explosive eruption phase. Early pyroclastic flow deposits are still strongly confined to palaeovalleys with a N-S to NNW-SSE orientation, suggesting a supply of material from point sources in the north. One example for these palaeovalleys can be seen in panel 2.2. where a fluvial valley (50 m width) was filled by several layers of pyroclastic density currents. The succeeding tuff layers however, have sheet-like appearances, indicating an accentuation of the former topography and steepening of the relief. Well preserved sedimentary organic matter (plant debris and palynomorphs; see Chapter 4) within the pyroclastic material points to relatively low depositional temperatures below 350°C (Stach et al., 1982). On top of the sections and panels, respectively, it can be seen that more fluvial material enters the system again. Mass flow deposits, being introduced from the north, indicate an increasing influence of a N-S trending volcanic induced alluvial-fan. This is documented by panels 2.5. and 2.6. showing the interfingering and successive progradation of the alluvial-fan into the underlying braided-river system.

Volcaniclastic deposits in Tepoztlán

North of Tepoztlán (18.99°N, 99.10°W) the thickness of the Tepoztlán Formation is about 380 m. One detailed stratigraphic section and two 2D-panels (one small scale and one large scale panel) were constructed in this area (Fig. 5). The volcaniclastic strata of the stratigraphic sections range in age from 21.8 to 18.8 Ma, belonging to the San Andrés and Tepozteco Member of the Tepoztlán Formation.

Stratigraphic section TEP

The Tepozteco section (TEP) is located north of Tepoztlán (Fig. 21). The thickness of this section is 378 m. The lower part is dominated by tuffaceous sandstones and conglomerates resulting from gravel bars and sandy channel fillings. Minor amounts of tuff such as the deposits of at least two block-and-ash flows can be recognized. The upper two thirds of the section are dominated by the deposition of coarse tuffaceous breccias, i.e. debris flow deposits resulting from lahars. The lahar deposits consist of a massive, matrix-supported breccia with angular to subangular, pebble- to cobble-sized clasts of andesite and dacite. It was not possible to ascertain the number of lahar deposits in a vertical sequence because distinct changes in sedimentology or erosional contacts were not apparent. Primary tuffs constitute only minor amounts in this part of the section. The volcaniclastic succession is locally capped by a 20 m thick dacitic lava flow. The top of the stratigraphic section is represented by more debris flow deposits with minor amounts of fluvial tuffaceous sandstones.

Small scale panel 3.1.

Representative for the mass flow dominated upper half of the section, panel 3.1. (Fig. 22) shows a succession of several stacked debris flow deposits. Only minor amounts of fluvial deposits can be found in this part of the sedimentary succession. The beds of matrix-rich breccia are up to 10 m thick, are inverse to normally graded and contain blocky, subangular clasts.

Large scale panel 3.2.

Panel 3.2. (Fig. 23), documents the change from a fluvial dominated to a mass flow dominated sedimentation within the sedimentary succession of the Tepoztlán Formation. The course of the stratigraphic section TEP is indicated by the red line.

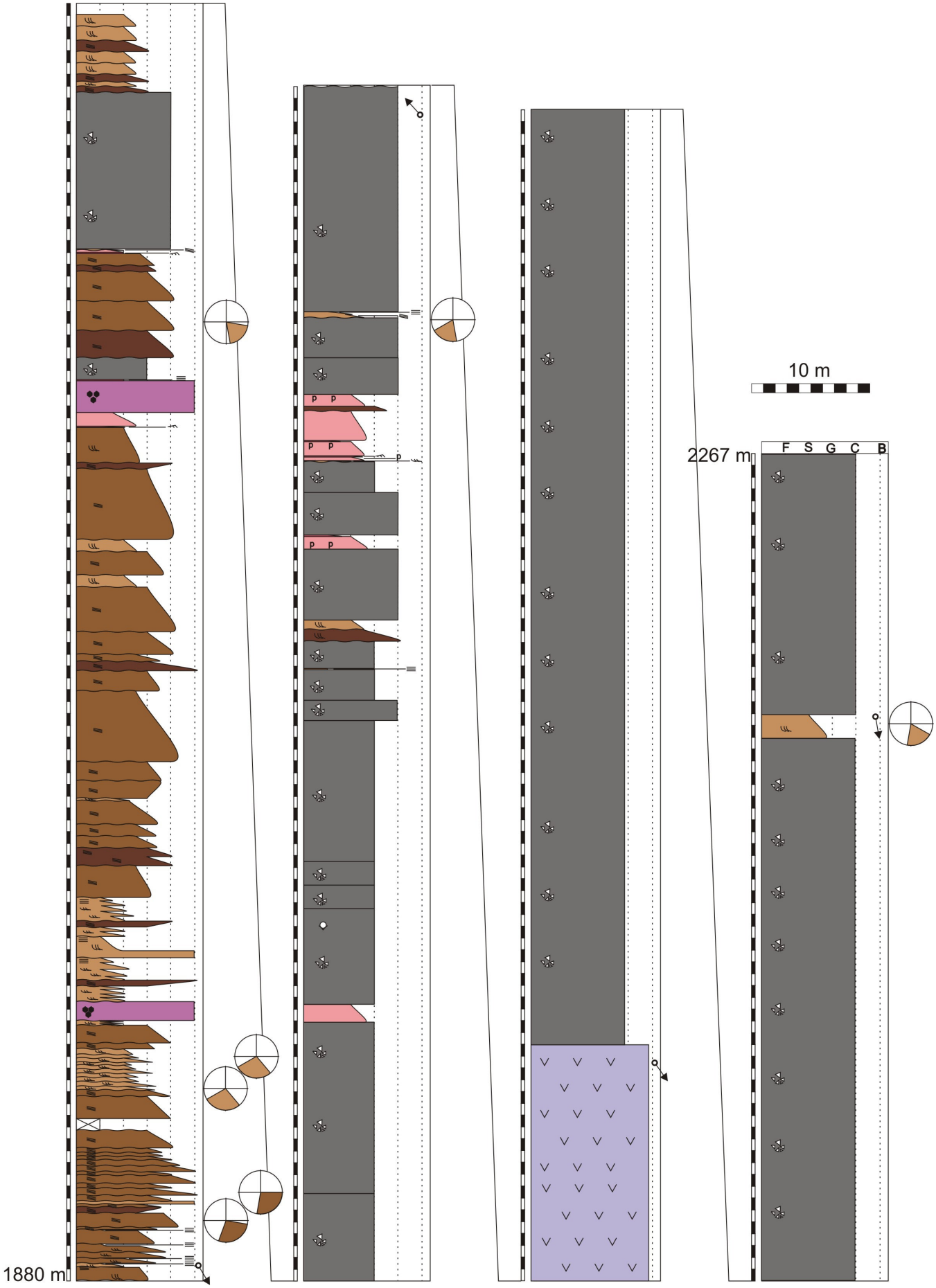

Figure 21. Lithostratigraphic section TEP of the Tepoztlán Formation near Tepoztlán (for legend see fig. 14).

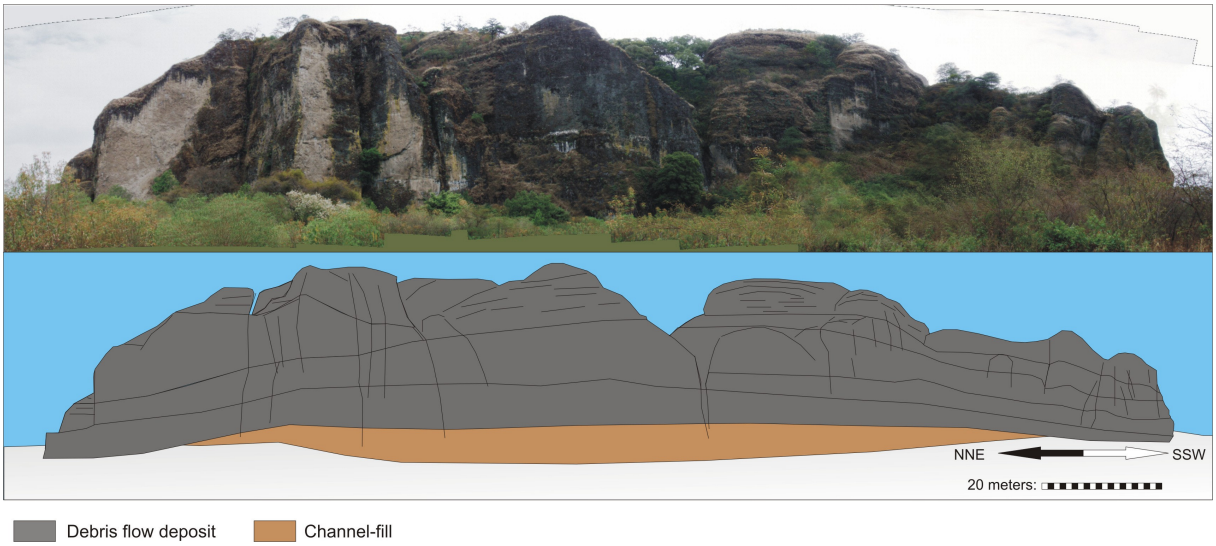

Figure 22. Small scale panel 3.1. (a) Photomosaic of the study outcrop. (b) Interpretation of the photomosaic.

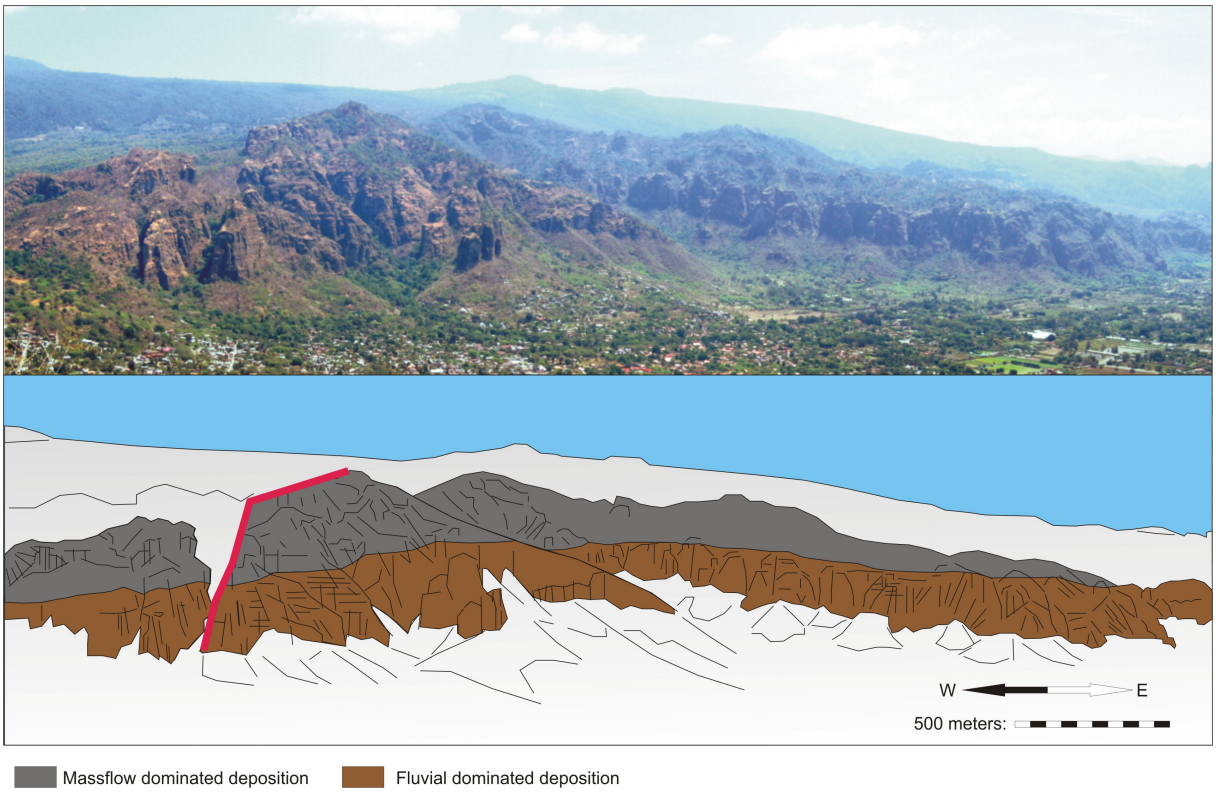

Figure 23. Large scale panel 3.2. (a) Photomosaic of the study outcrop. (b) Interpretation of the photomosaic. The red line indicates the course of the stratigraphic section TEP.

Interpretation

The characteristics of the sedimentary facies and bed geometry in the lower part of the sedimentary succession of the Tepoztlán Formation, documented in this location, indicate that the system was dominated by stream floods of high competence to transport even boulder-size

clasts. This is documented by the dominance of amalgamated bouldery conglomerates, tuffaceous sandstones and thin bedded tuff and tuff breccia deposits. The predominance of low-angle erosional surfaces, small bouldery bars, and relatively thin sandy channel-fills supports deposition in a system of shallow migrating channels with longitudinal bars and unstable banks characteristic for a high-energy braided river system. Bouldery conglomerates at the base of channels are interpreted to be lag deposits. All clasts within the fluvial deposits are of volcanic origin. The sandy matrix is probably due to reworking of unlithified ash. This shows that the volcanic activity is still ongoing within the study area and regularly introduces fresh, unlithified volcanic material into the stream. Direct evidence for the volcanic activity is the relatively thin pyroclastic flow deposits. Block-and-ash flow deposits represent a near-vent facies and show the proximity to the source area, not more than 5 or less km away from the place of deposition (Williams and McBirney, 1979). With higher elevations, the fluvial sediments are suddenly replaced by a massive stack of debris flow deposits, resulting from lahars, dominating the sedimentary succession to the top. The debris flows are inferred to have been produced by relatively near-source reworking of vent-facies lava flows and pyroclastic material. The abundance of channelized to unchannelized mass flow deposits is commonly indicative of small coalescing alluvial-fans with high angles of repose and restricted catchments (Nemec and Postma, 1993). The lack of fluvial sediments suggests that the post-depositional fan incision was limited. The volcaniclastic sequence is capped by a thick dacite flow, indicating near-vent facies and suggesting a decrease in eruption intensity and a transition from explosive to effusive activity. However, the succession is completed by the deposition of further debris flow deposits, pointing to a new flare-up of explosive volcanic activity. However, pyroclastic flows could not reach far enough anymore to leave any remains or were reworked by mass flow processes immediately after deposition and leaving no trace of primary deposits. Another explanation for the huge packages of mass flow deposits can be deposition in a phase of edifice destruction and thus the final stage within the evolution of the Tepoztlán Formation.

Volcaniclastic deposits of the Cerro Sombrerito (Tlayacapan)

West of Tlayacapan (18.94°N, 98.98°W) the Tepoztlán Formation attains a thickness of about 200 m. Two detailed stratigraphic sections and three 2D-panels were constructed in this area (Fig. 5). The volcaniclastic strata of the stratigraphic sections range in age from 22.2 to 20.1 Ma, belonging to the San Andrés and Tepozteco Member of the Tepoztlán Formation.

Stratigraphic sections SO1 and SO2

The Sombrerito 1 section (SO1), southwest of Tlayacapan reaches a thickness of 78 m (Fig. 24). The basis of the section forms an about 24 m thick lava flow. The lava flow is formed by a dense core and a blocky carapace. On top of the flow we can see a thickening- and

coarsening-upward sequence of tuffaceous sandstones and conglomerates. Minor tuffs of a few 10s of centimetres in thickness occur in regular intervals all throughout the entire stratigraphic section. After a huge scour 2 m of sandy, horizontally to low-angle cross-bedded sheet flood sediments are documented on top of a thin pyroclastic flow deposit. Sandy channel elements are more and more decreasing to the top from here whereas an increase in coarse gravel bars and scours can be noticed. Debris flow deposits occur occasionally.

The Sombrerito 2 section (SO2), is a continuation of SO1 but with a horizontal shift of 100 m towards northwest and attains a thickness of 110 m. In the lower part it is mostly composed of primary volcanic products resulting from pumice-and-ash and block-and-ash flows. With increasing altitude coarse fluvial deposits in the form of gravel bars become more and more dominant with increasing amounts of mass flow deposits to the top.

Small scale panel 4.1.

The small scale panel 4.1. represents the dominating fluvial deposits in the lower part of the sedimentary succession at the Cerro Sombrerito (Trauth, 2007). In the right part, two sandy channel-fills, showing normal grading, can be seen at the base of the panel (Fig. 25). On top of this element, an about 1 m thick gravel bar follows. The gravel bar consists of moderately rounded cobbles and blocks in a sandy matrix. The top of the bar shows signs of erosion and scouring. The gullies and small channels are filled with fine, normally graded sands. These sediments are again covered by another stack of gravely bar deposits, showing planar crossbedding and imbrication of their cobbly clasts. Finally, another channel can be found on top of the gravels, eroding them at the base and entraining them into the sandy deposits above.

Medium scale panel 4.2.

The medium scale panel 4.2. has a N-S orientation (Fig. 26). The base consists of predominantly flat-lying tuffaceous sandstones which are interpreted as sandy channel-fills. Sedimentary features of the channel indicate a E-W to NE-SW flow direction of the stream. Single layers are between 1 and 3 m thick. In the upper half of the panel, coarse gravel bars are increasing which are getting thicker to the top. Simultaneously, an increase of debris flow elements is recorded. Tuffs of pyroclastic flow elements can be found in relatively regular intervals. However, they are more abundant in the lower half of the panel.

Medium scale panel 4.3.

More to the north and on the opposite side of the mountain range, close to the village of Santo Domingo (19.00°N, 99.03°W; Fig. 27), a similar pattern of the sediments as described in panel 4.2. within the succession can be seen. The panel has N-S orientation and it can be seen that the fluvial sediments are dominated by coarse gravels, deposited by gravel bars. In the left part a relatively wide fluvial channel (400 m width) with E-W orientation can be seen which is filled up by lahar deposits. These mass flow deposits are partly eroded again by

fluvial deposits to the right, forming a new channel within the tuffaceous breccias below. However, this channel is filled by the tuffs of a pyroclastic flow and by at least 5 m thick lacustrine sediments, formed a lake of at least 200 m width. On top of the lacustrine silt- and claystones, more gravely fluvial deposits can be found. However, in the upper half of the panel, fluvial deposits are strongly decreasing while more and more mass flow deposits enter the system from the north.

Large scale panel 4.4.

The large scale panel 4.3. (Fig. 28) shows the dominating sedimentary systems over the entire length of the N-S trending mountain range west of Tlayacapan. The locations of the small scale panel 4.1. and the medium scale panel 4.2. are indicated. Fluvial sedimentation dominates in the lower part of the panel and especially in the south. In the north, mass flow processes seem to have an increasing influence on the sedimentation in the upper part of the succession.

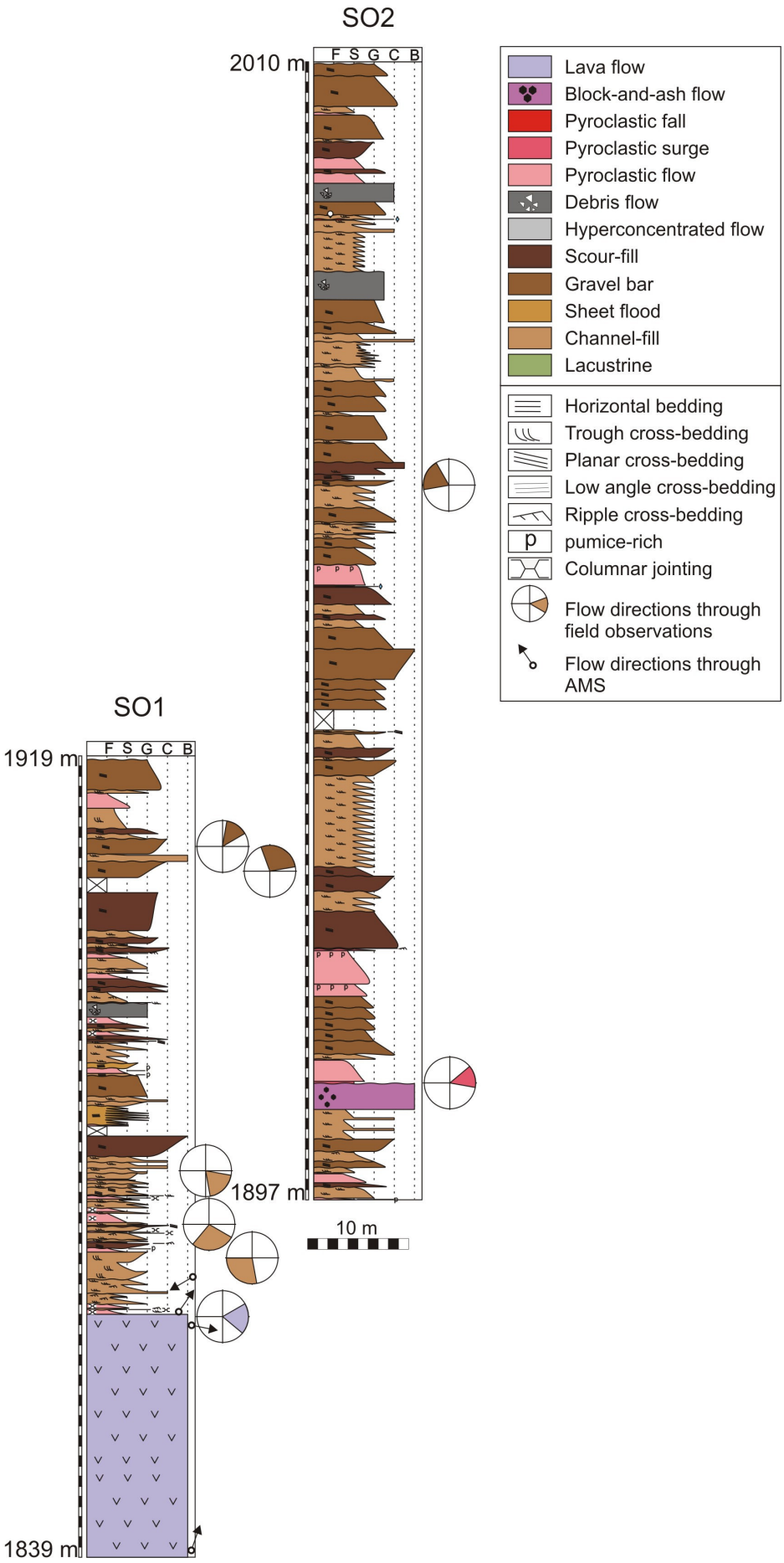

Figure 24. Lithostratigraphic sections SO1 and SO2 of the Tepoztlán Formation near Cerro Sombrerito.

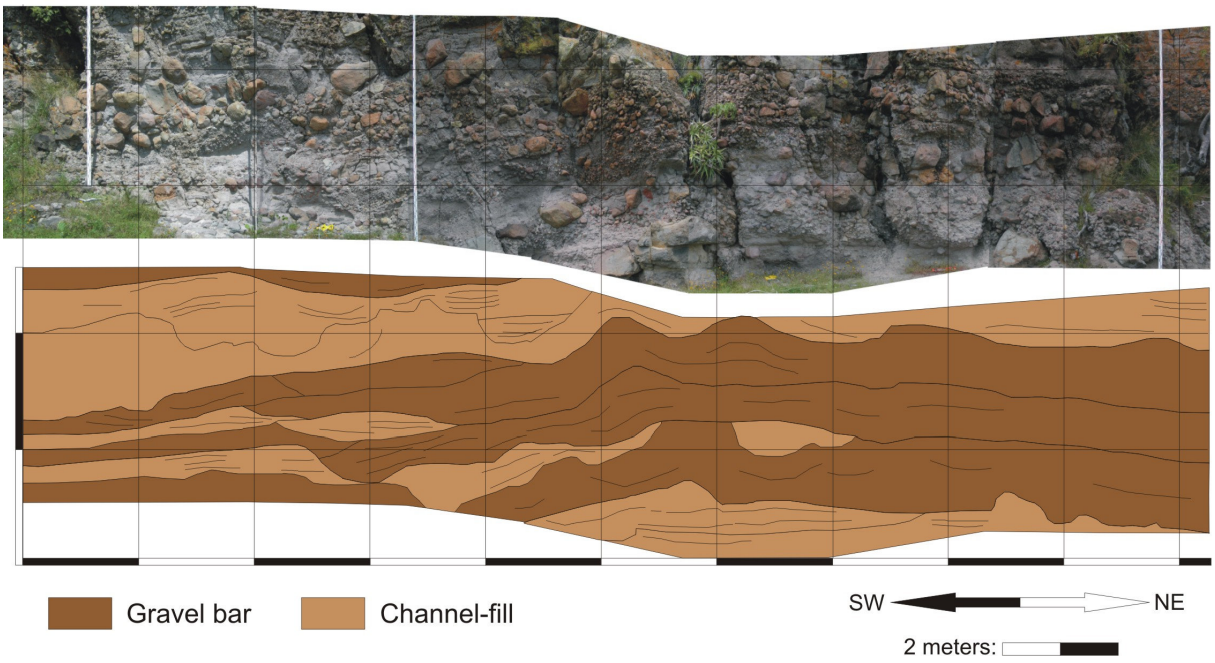

Figure 25. Small scale panel 4.1. (a) Photomosaic of the study outcrop. (b) Interpretation of the photomosaic.

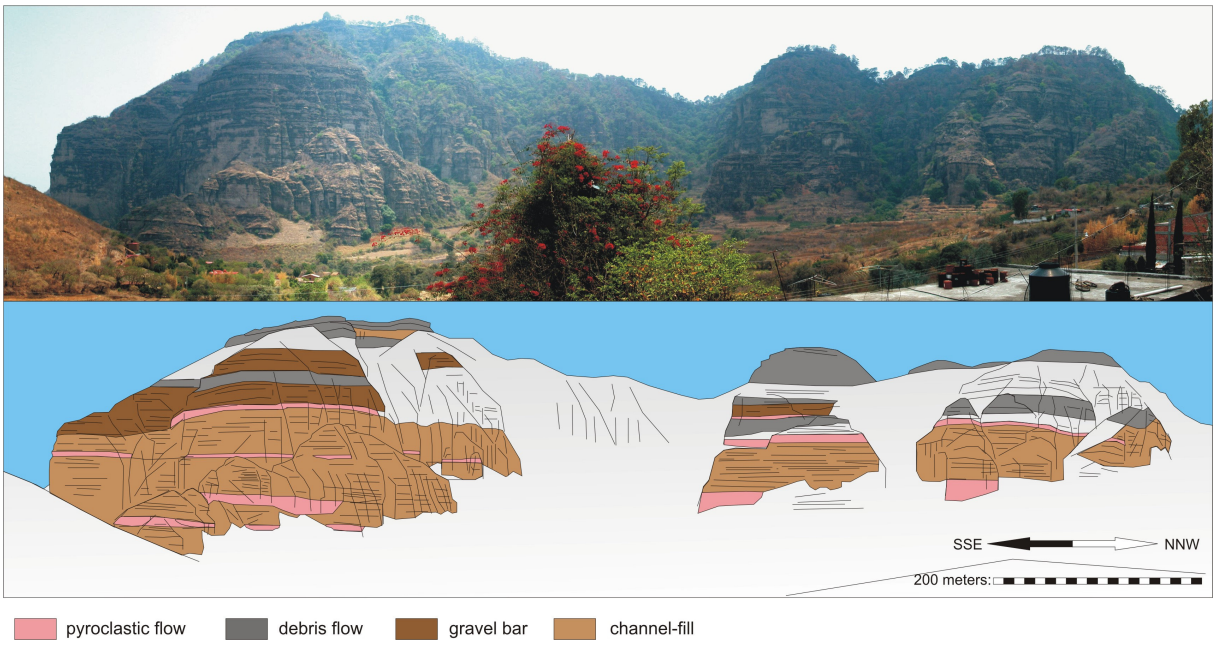

Figure 26. Medium scale panel 4.2. (a) Photomosaic of the study outcrop. (b) Interpretation of the photomosaic.

Figure 27. Large scale panel 4.3. (a) Photomosaic of the study outcrop. (b) Interpretation of the photomosaic.

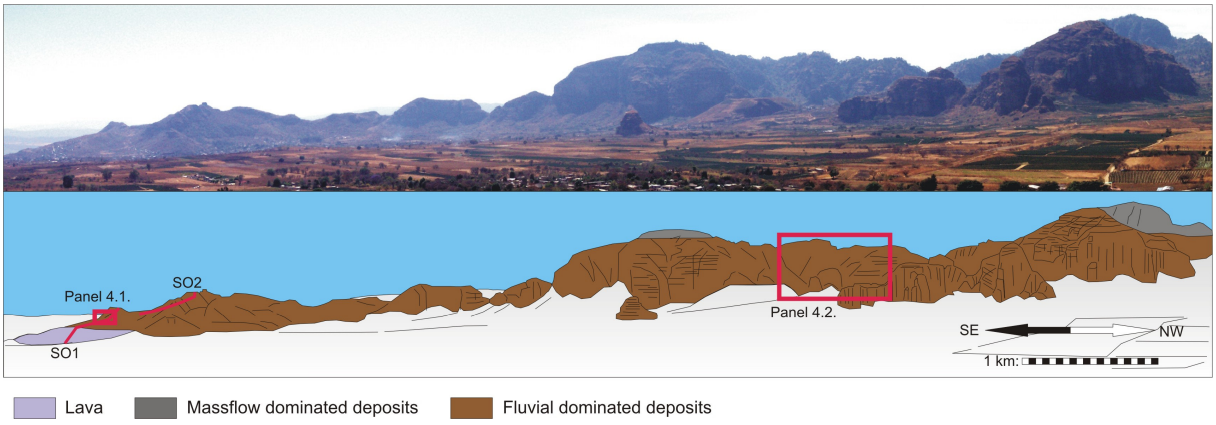

Figure 28. Large scale panel 4.4. (a) Photomosaic of the study outcrop. (b) Interpretation of the photomosaic. The red lines indicate the courses of the sections SO1 and SO2. The red frames indicate the locations of the 2D-panels 4.1. and 4.2.

Interpretation

The deposition of a thick lava flow at the base of the sedimentary succession in this location indicates a high effusive volcanic activity. The lava flow is interpreted as near-vent facies, proximal to the source area. In the following time, the effusive activity was replaced by more explosive volcanism. This is shown by the deposition of several pyroclastic flows on top of the lava. However, only thin layers of these primary tuffs remained due to strong reworking of

the material by streams. The fluvial material, derived from reworked unlithified ash, forms small channels which incise and overlap one another. This suggests a deposition in a shallow braided-river system of low competence and relatively low energy. Bouldery conglomerates at the bottom of few channels are interpreted as lag deposits. Higher up in the succession we notice an increase of flow energy. The sheet-flood elements (see stratigraphic section SO1) are interpreted as high-energy deposits. Sheet-floods are often formed at the transition from proximal to distal alluvial fans (Orton and Reading, 1993). Together with the occurring mass flow deposits, they indicate the interfingering and successive progradation of an alluvial-fan into the braided-river system. Following these sediments an increase in coarse gravely material, deposited by gravel bars and scours, is documented. The small gravel bars and scours together with the sandy channel-fills support a deposition in a system of shallow migrating channels with longitudinal bars and unstable banks. The increase of these gravel bars, in combination with a coarsening- and thickening-upward trend within the succession points to a successive increase in flow energy and competence of the stream. They are furthermore interpreted as a steepening of the relief in an aggradational setting. By means of the imbrication of the clasts with the gravel bars a palaeocurrent direction from NE to SW (see small scale panel 4.1.) can be proposed. The material is very immature and the clasts are often poorly rounded. Hexagonal shapes give evidence that many clasts are derived from reworked block-and-ash flows. As described in the other locations before, the regular intervals of occurrence of the pyroclastic flow deposits points to explosive volcanic activity in regular points of time. The block-and-ash flow deposits, which can be observed in stratigraphic section SO2, are interpreted as near-vent facies and are a sign for ongoing volcanic activity close to the area of deposition. This is supported by the deposition of massive ignimbrites of top and the occurrence of surge deposits with antidune structures. Following these primary volcanics an increase of fluvial deposits is documented. Primary volcanics are subordinate. However, they still occur in relatively regular intervals, pointing to regular eruptive activity. The fluvial deposits, mostly coarse gravel bar elements with minor channel and subordinate scour elements show a coarsening- and thickening-upward trend to the top and are evidence for a progress in the steepening of the relief, related to the progradation of an alluvial-fan. In the medium scale panel 4.3., a fluvial channel of several 10s of meters in width can be recognized which is interpreted to be one of the main channels of the braided river. The channel is filled up with the deposits of at least one massive debris flow and a pyroclastic flow. The clayey and silty, fine laminated sediments on top are interpreted as lacustrine deposits due to river damming. In the southern part debris flow elements interfere towards the top increasingly with gravel bars whereas they are dominating in the north pointing to a N-S flow direction of the volcanic induced alluvial-fan.

Volcaniclastic deposits of the Cerro Tonantzin (Tlayacapan)

The Cerro Tonantzin (18.58°N, 98.59°W) is a small hill NE of Tlayacapan and SW of San Agustín. One detailed stratigraphic section and three 2D-panels (one small scale panel and two medium scale panels) were constructed in this area (Fig. 5). The volcaniclastic strata of the stratigraphic sections range in age from 22.2 to 20.1 Ma, belonging to the San Andrés and Tepozteco Member of the Tepoztlán Formation.

Stratigraphic section TO

The Tonantzin section (TO), in the northeast of Tlayacapan has a thickness of 79 m (Fig. 29). While tuffaceous sandstones resulting from sheet-floods and sandy channel-fills are dominating in the lower part of the section, tuffaceous conglomerates in the form of gravel bars are becoming increasingly important in the upper part of the section. Simultaneously, deposits resulting from pumice-and-ash flows and debris flows are becoming more increasingly abundant to the top.

Small scale panel 5.1.

The small scale panel 5.1. (Fig. 30) shows the interfingering of different facies types and thus, depositional processes, in very limited time and space. The base of the panel is characterised by sediments of a hyperconcentrated flow which is subsequently followed by the pebbly layer of a gravel bar. The moderately rounded pebbles show imbrication. A second hyperconcentrated flow deposit follows on top. Single outsized clasts of about 40 cm in diameter can be found within that layer as well as little pumice particles. The following sheet flood elements show horizontal bedding and are about 10 cm thick each. These sediments can be traced throughout the entire panel. On top of the sheet flood elements a sandy channel-fill element can be seen. A scour-fill element carves deep into these sediments below into the hyperconcentrated flow deposit. Following this, a stack of overlapping gravel bars can be seen. Two about 2 m thick pyroclastic flow deposits are intercalated between the tuffaceous conglomerates and can be traced throughout the panel. On top of the stack of gravel bars is another hyperconcentrated flow deposit which is covered by sheet flood elements. There are signs for layers of pyroclastic fall elements within these sediments. However, the major part is lacking due to erosion by the sheet flood. Sandy channel-fill elements are dominating in this part of the panel while the importance of gravel bars is decreasing. Another ignimbrite sheet follows on top of the channel sediments and can be traced over the entire panel, followed by another stack of sheet flood elements before the channel elements reappear.

Medium scale panel 5.2.

The medium scale panel 5.2. documents the continuation of the small scale panel 5.1 (Fig. 31). Sandy channel-fill and sheet flood elements dominate at the base of the panel. Higher up in the panel, the coarser conglomerates of gravel bars become more important while finer-

grained channel elements are decreasing. Simultaneously, there is an increase in mass flow deposits, first in hyperconcentrated flow, later in debris flow elements. Pyroclastic flow deposits can be traced through the panel in regular intervals.

Medium scale panel 5.3.

The medium scale panel 5.3. shows the other side of the hill, opposite to 5.2. and thus enables to analyse the sedimentary succession in the location from all sides (Fig. 32). The observations of 5.1. and 5.2. are comprehensible in this panel. There is a dominance of coarse gravel bars in the lower third of the panel which is succeeded by several sheet floods and intercalated pyroclastic flow deposits. Following these sediments, channel-fill elements become increasingly important, disrupted by occasional sheet flood or gravel bar elements. In the upper third of the section, another increase of gravel bar and debris flow deposits can be noticed.

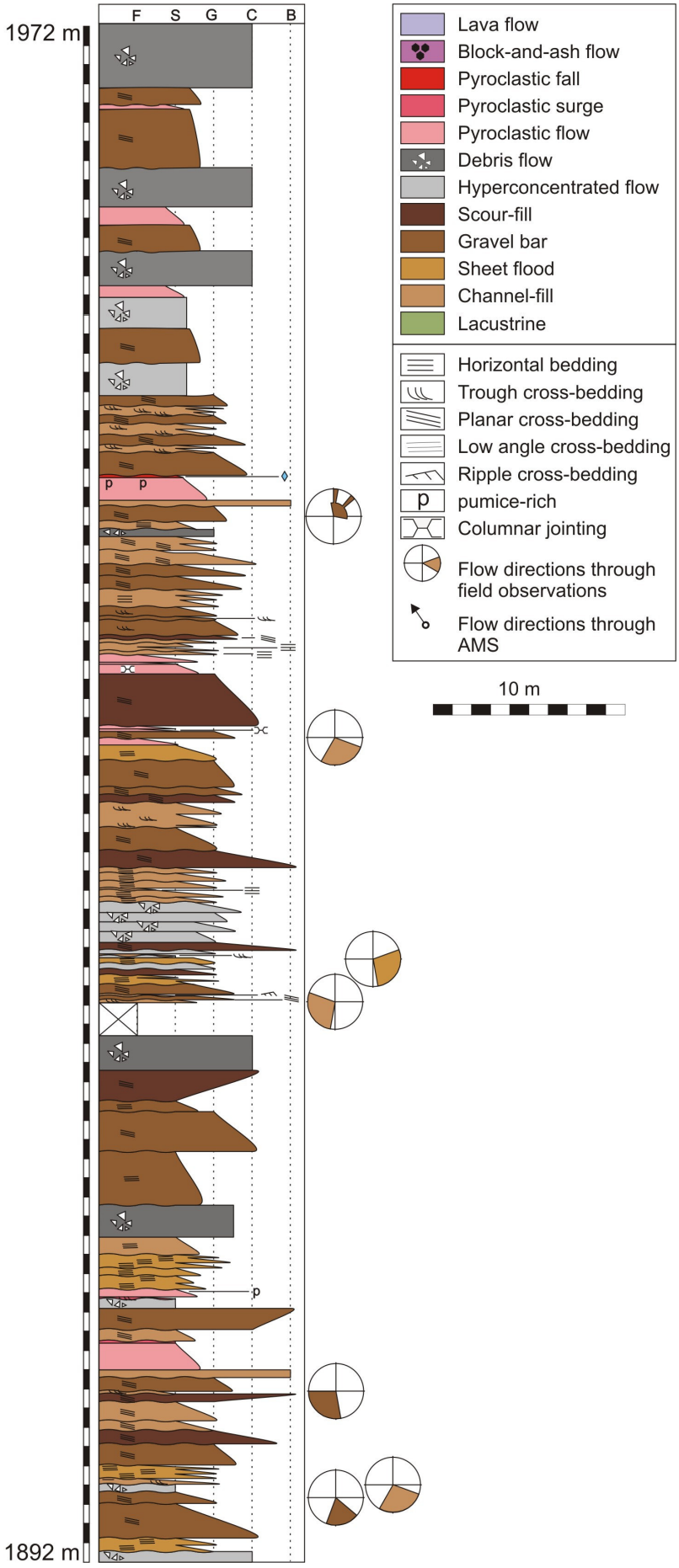

Figure 29. Lithostratigraphic section TO of the Tepoztlán Formation near Cerro Tonantzin.

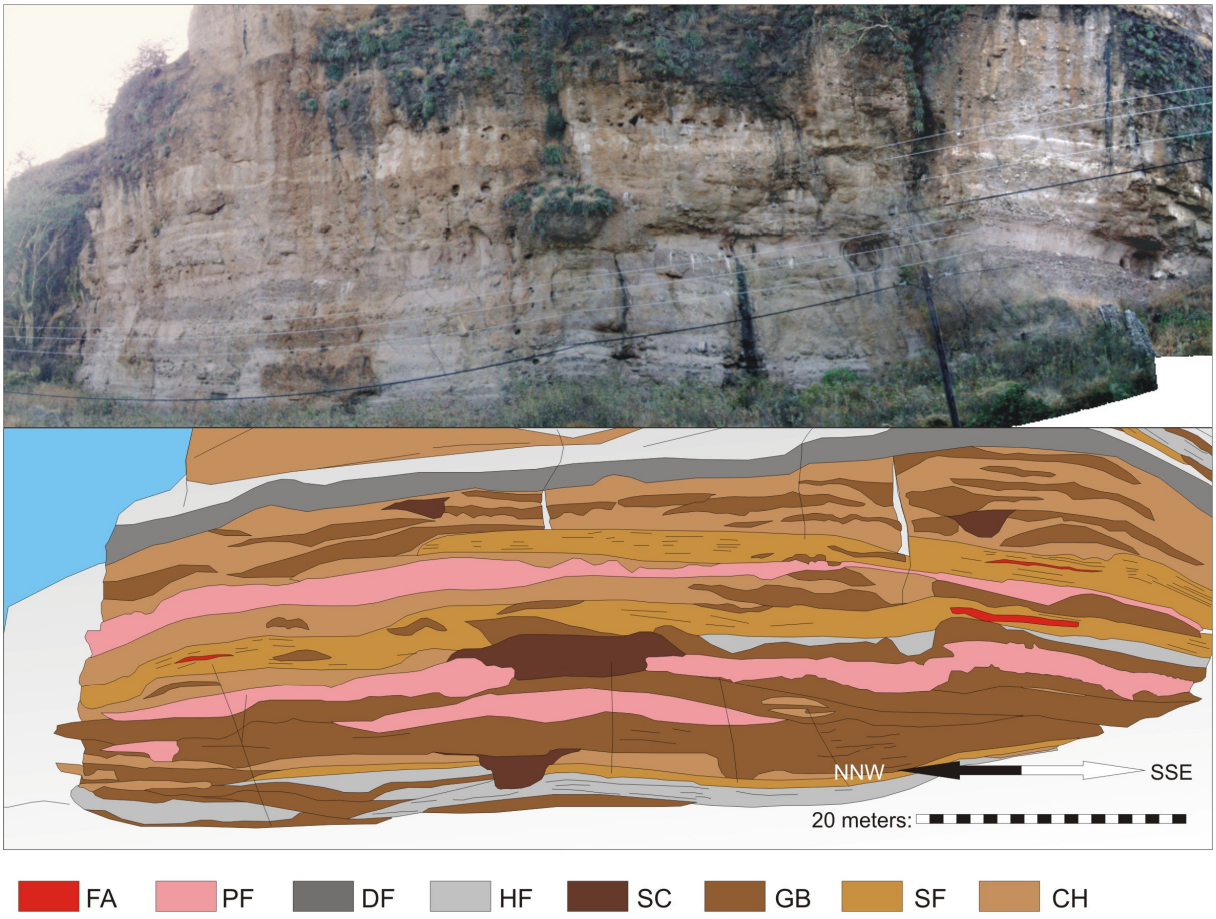

Figure 30. Small scale panel 5.1. (a) Photomosaic of the study outcrop. (b) Interpretation of the photomosaic. FA, pyroclastic fall; PF, pyroclastic flow; DF, debris flow; HF, hyperconcentrated flow; SC, scour-fill; GB, gravel bar; SF, sheet flood; CH, channel-fill.

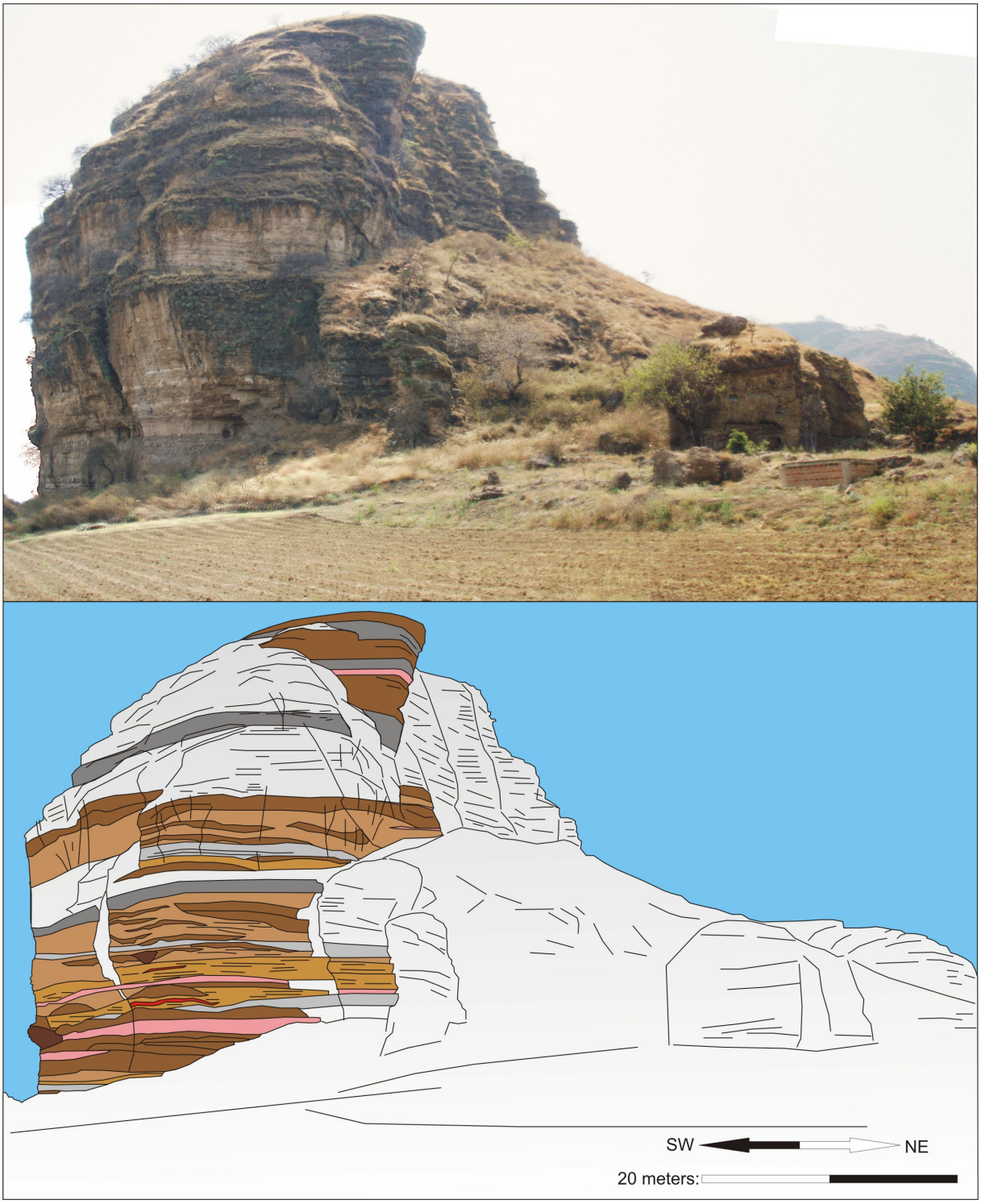

Figure 31. Medium scale panel 5.2. (a) Photomosaic of the study outcrop. (b) Interpretation of the photomosaic. FA, pyroclastic fall; PF, pyroclastic flow; DF, debris flow; HF, hyperconcentrated flow; SC, scour-fill; GB, gravel bar; SF, sheet flood; CH, channel-fill.

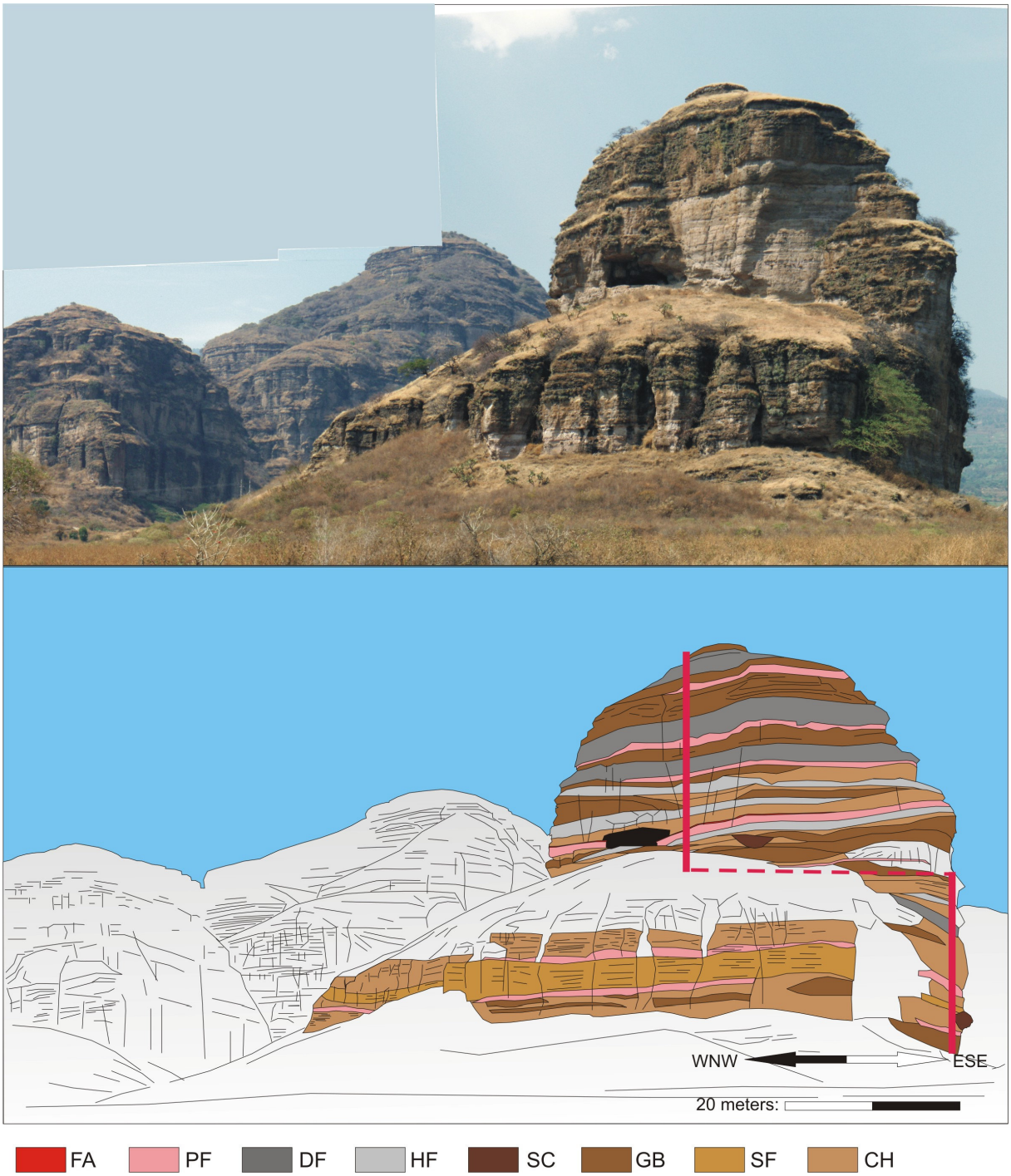

Figure 32. Medium scale panel 5.3. (a) Photomosaic of the study outcrop. (b) Interpretation of the photomosaic. FA, pyroclastic fall; PF, pyroclastic flow; DF, debris flow; HF, hyperconcentrated flow; SC, scour-fill; GB, gravel bar; SF, sheet flood; CH, channel-fill. The red line indicates the course of the stratigraphic section.

Interpretation

The base of this location is characterized by the deposition of several hyperconcentrated flows. The deposits of these highly sediment charged flows are normally easily eroded during floods. In this location, the eroded sediment was unlithified volcanic ash which was entrained after initial volcanic eruptions in the hinterland. Usually, hyperconcentrated flows are

considered to be the distal run-out flows of lahars, resulting from mass flow processes on a volcanic induced alluvial fan. The hyperconcentrated flow deposits are intertwined with coarse gravel bar elements. The occurrence of the gravel bars as small overlapping longitudinal bars suggests a deposition in a braided river system with shallow migrating channels. The imbrication of the clasts indicates a palaeocurrent direction from NE to SW. In the upper part of small scale panel 5.1., pyroclastic flow elements enter the fluvial system and are partly eroded and reworked by the gravel bars. The increasing volcanic activity causes an enhancement in sandy tuffaceous material that is deposited in channel elements. Sheet floods, the distal sediments of alluvial fans are now occurring more often, indicate the growing of a fan system in the hinterland. Layers of pumice lapilli in between the sheet flood elements are a sign for pumice falls suggesting subplinian to plinian eruptions simultaneous to the deposition of the sheet flood sediments. Due to an increase of ash an increase of channel elements is documented, intertwined with subordinate gravel bars and scour elements. Sediments resulting from mass flow processes, debris flow or hyperconcentrated flow deposits interrupt the fluvial sedimentation in regular intervals. Similarly, regular intervals of pyroclastic flow deposits point to regular times of explosive volcanic activity. This regularity of occurrence of mass flows and primary volcanic material proceeds up to the top of the succession in this location. However, debris flow deposits are slightly increasing. In the upper half of the succession, a renewed increase of gravel bars elements is recorded together with a coarsening- and thickening-upward trend. This is interpreted to be the result of a steepening of the relief along with a higher flow energy caused by a stronger influence of a growing alluvial fan system in proximal to median distances.

Volcaniclastic deposits of San Agustín

North of the village San Agustín (18.99°N, 98.96°W) the Tepoztlán Formation attains a thickness of about 133 m. One detailed stratigraphic section and two medium scale 2D-panels were constructed in this area (Fig. 5). The volcaniclastic strata of the stratigraphic sections range in age from 20.1 to 19.0 Ma, belonging to the Tepozteco Member of the Tepoztlán Formation.

Stratigraphic section TL

The San Agustín section (TL) is located northeast of Tlayacapan and just north of San Agustín village. It attains a thickness of 133 m and is characterised by a steady increase in pyroclastic flow deposits (Fig. 33). Deposits from debris flows are abundant whereas fluvial tuffaceous sandstones and conglomerates decrease with increasing altitude within the section. The top of the section is characterised by a thick, blocky lava flow.

Medium scale panel 6.1.

The medium scale panel 6.1. shows the sedimentary succession of the Tepoztlán Formation in San Agustín with SSW-NNE orientation (Fig. 34). The course of the stratigraphic section TL is indicated as a red line. The base of the panel is characterised by a hyperconcentrated flow and a stack of amalgamated gravel bars. Following the massive breccia of a debris flow element, the deposits of several pyroclastic flows and falls fill up an erosional valley. The upper PF elements are sheet-like and can be traced throughout half of the panel. On top of these thick and massive ignimbrites, channel fills are the dominating architectural elements while gravel bars occur only occasionally. On top of these fluvial sediments, primary volcanics are increasing again. After a debris flow element, the deposits of a block-and-ash flow and at least three about 2 - 4 m thick pyroclastic flows can be noticed. Following the stack of primary volcanics, fluvial sediments are dominating again. The fluvial sediments predominantly consist of stacked channel elements with subordinate gravel bars. In the middle part of the panel we document an at least 150 m wide erosional surface within the fluvial deposits that we interpret as a palaeoriver valley. The base of the valley is characterised by deposition from a pyroclastic flow. It is filled up by sandy channel elements. The top of the panel is characterised by thick pyroclastic flow elements that it capped by a blocky dacitic lava flow.

Medium scale panel 6.2.

The medium scale panel 6.2. (Fig. 35) shows the opposite side of 6.1. with a NNE-SSW orientation. The description of 6.1. is still comprehensible on this side. The lower part is characterised by gravel bars that are followed by a massive thick debris flow and a stack of deposits of at least four pyroclastic flows. On top of the stack of primary volcanics, the next 15-20 m are dominated by sandy channel fills. Within the fluvial sediments a depression of about 150 m in width and a WNW-ESE orientation is documented, probably the same one which was already described as a palaeoriver valley in 6.1., before. The base of its filling is characterised by the deposition of a pyroclastic flow deposit. The remaining mould is filled up by sandy channel sediments. It is covered by two thick sheets of pyroclastic flow elements. The next 15-20 m are dominated by small overlapping channel elements again with only subordinate gravel bars. However, gravel bars are slightly increasing to the top. Furthermore, the deposition of at least two thick debris flows can be documented. Again, the top of the panel is finally dominated by pyroclastic flow elements with subordinate channel elements. The very top of the panel is characterised by a blocky lava flow.

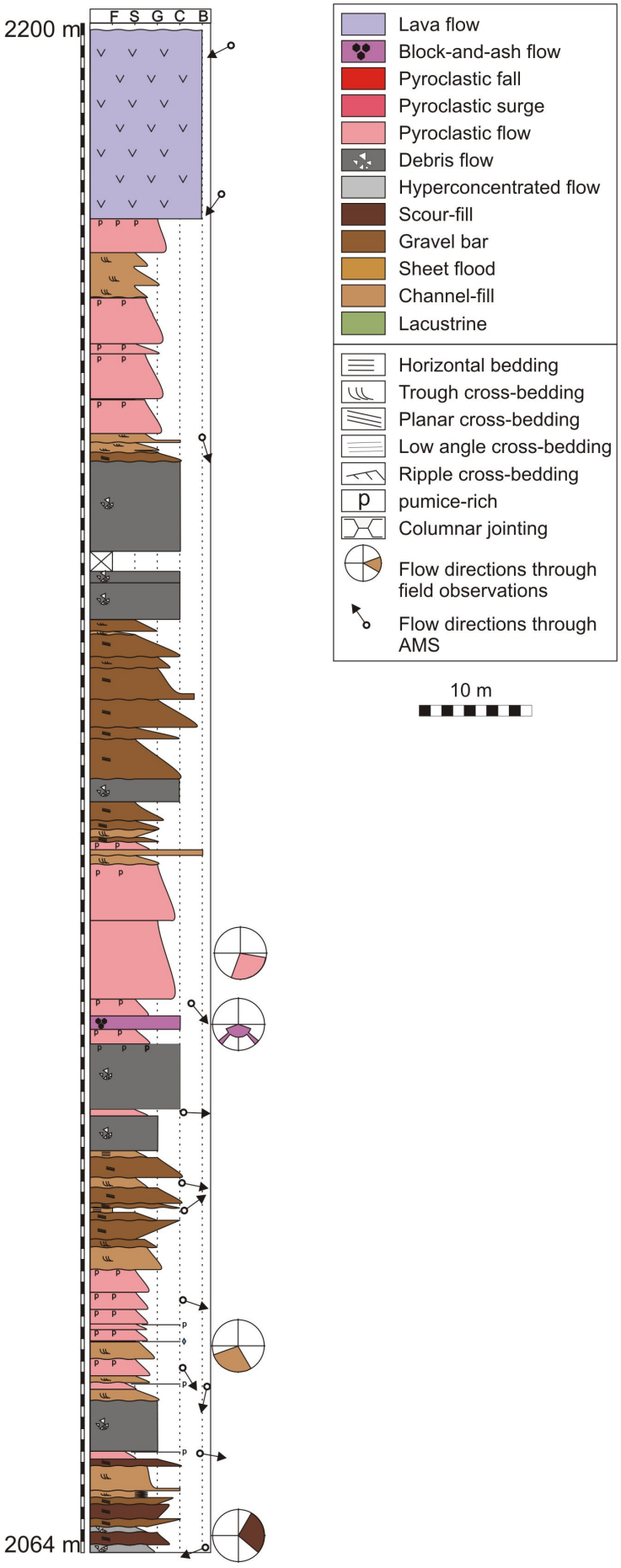

Figure 33. Lithostratigraphic section TL of the Tepoztlán Formation near San Agustín.

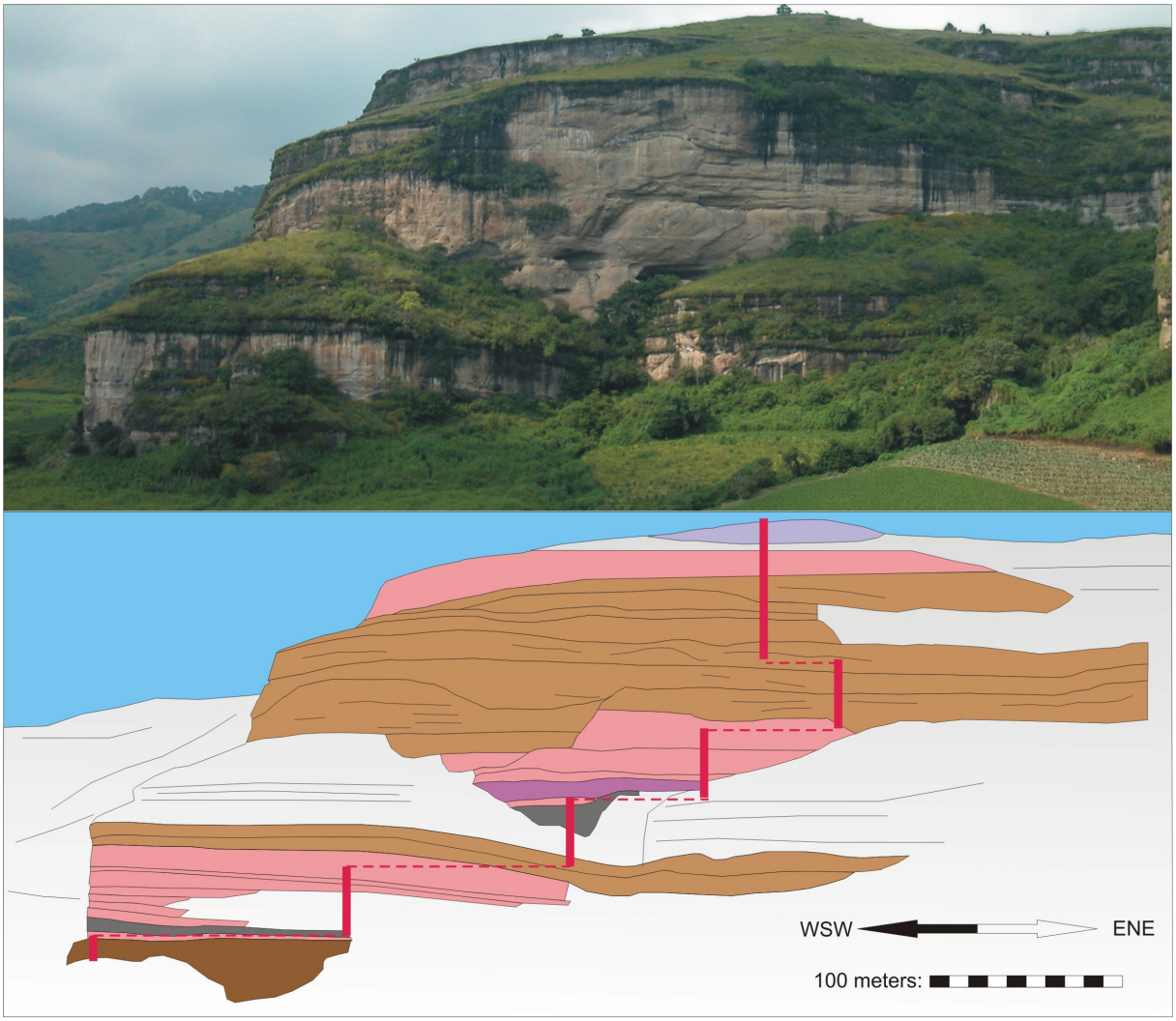

Figure 34. Medium scale panel 6.1. (a) Photomosaic of the study outcrop. (b) Interpretation of the photomosaic. PF, pyroclastic flow; BA, block-and-ash flow; DF, debris flow; GB, gravel bar; SF, sheet flood; CH, channel-fill. The red line indicates the course of the stratigraphic section TL.

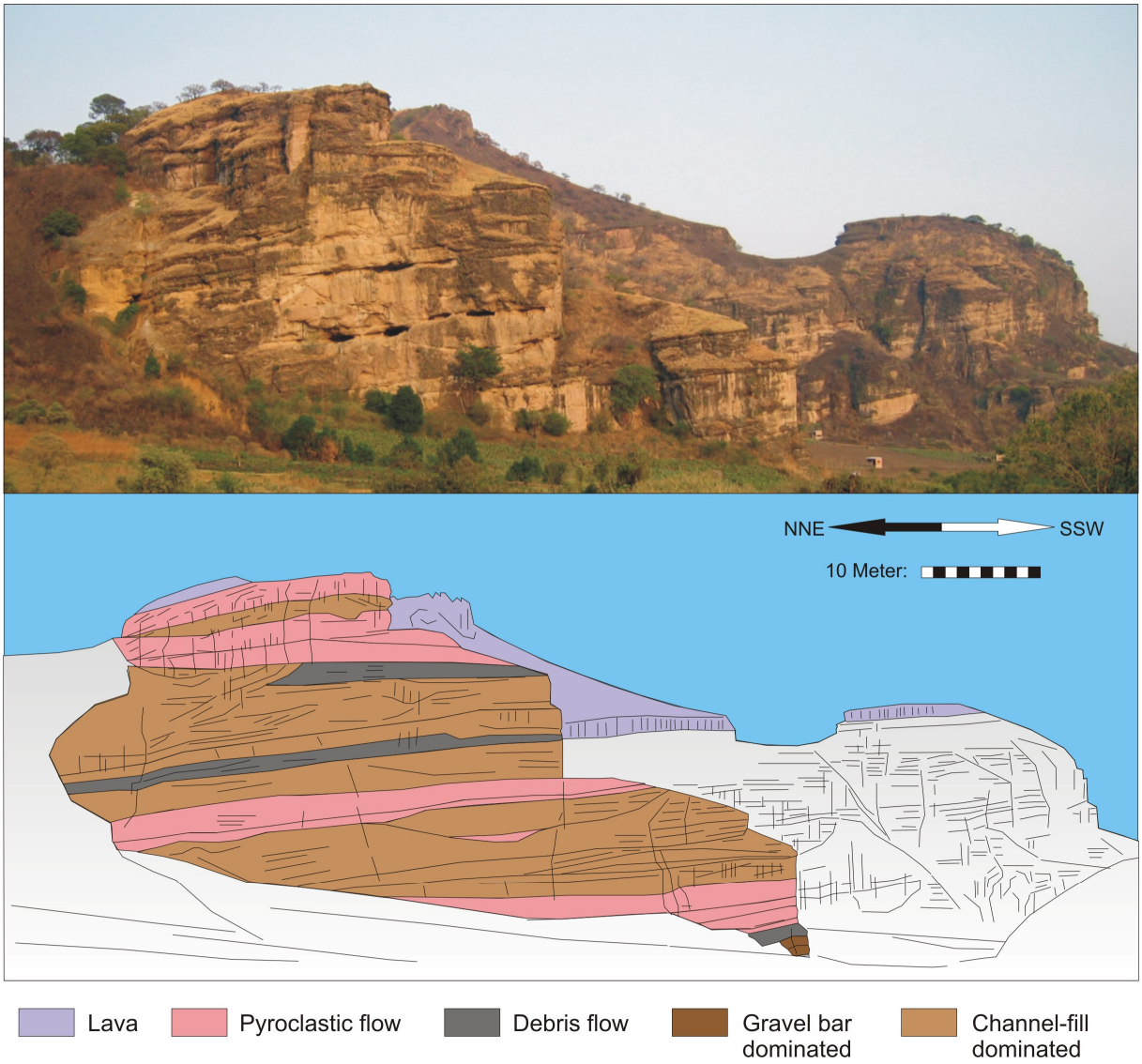

Figure 35. Medium scale panel 6.2. (a) Photomosaic of the study outcrop. (b) Interpretation of the photomosaic.

Interpretation

The basis of the sedimentary succession in this location is characterised by the deposition of hyperconcentrated flows, intertwined with gravel bars, scours and several overlapping channel elements in a setting that is interpreted to be a braided river system. As already described in chapter 6.5., the hyperconcentrated flow deposits can form as distal parts of lahars when large quantities of unlithified ash are transported down the slope of an alluvial fan. The following coarse debris flow and pyroclastic flow deposits, both proximal to median facies, however, suggest that the hyperconcentrated flows formed due to dilution when debris flows were entrained into the stream. A 12 m thick stack of pyroclastic flows and falls of micropumice, intercalated with fluvial sediments and filling up a fluvial channel, indicate a period of high explosive activity. Following these deposits, an inter-eruptive period with an increase in coarse gravel bars and minor channel elements can be documented. This is followed by another phase of high volcanic activity. Similar to the locations described before,

continuous pattern in the occurrence of primary volcanic material, being exposed every 20 – 30 m, is documented. Two thick debris flow deposits and another 15 m thick stack of pyroclastic flow deposits on top of the gravel bar dominated zone are interpreted to indicate an increasing influence of a volcanic induced alluvial fan. Especially the deposition of a block-and-ash flow deposit within the ignimbrites suggests a proximal distance to the volcanic source area. Presumably, it was formed due to a lava dome collapse only a few km from its place of deposition. The block-and-ash flow was partly eroded and the dense blocks were entrained by the following ignimbrite. The medium scale panel 6.1. shows the erosion of a deep river valley with WNW-ESE orientation into the pyroclastic sediments in the south. The valley was filled up by sandy channel elements and minor pyroclastic flows. The same valley can be documented at the other side of the location in panel 6.2. Here, it can be interpreted as the main channel of a river with WNW-ESE orientation. The mostly sandy channel deposits are followed by an increase of gravel bars, showing a coarsening- and thickening-upward trend. The deposition of fluvial sediments is finally interrupted by thick debris flow elements and another 20 m thick stack of pyroclastic flow deposits. The pyroclastic flow elements are intercalated with minor fluvial sediments, mostly sandy channel elements. The dacitic lava flow on top of the volcaniclastic succession is interpreted as near-vent facies and marks a change from explosive to effusive volcanism in this location.

4.2.4. palaeocurrent analysis

Field observations

The palaeocurrent direction was measured from various sedimentary structures, i.e. clast imbrication, trough cross-stratification (from three-dimensional exposure) and the shape of scours and channels (see lithostratigraphic sections). Palaeocurrent directional data are commonly used to interpret channel sinuosity. A low dispersion in the palaeocurrent values is consistent with a low-sinuosity or braided stream interpretation (Bridge, 1985). A higher dispersion of values can indicate deposition in higher sinuosity or meandering stream settings (Bluck, 1971). Within the Tepoztlán Formation, a total of 156 palaeocurrent directions were taken. The mean transport direction of the fluvial deposits of the Malinalco Member was to the east with a circular standard deviation of 49° (Fig. 36). Measurements on bomb sag structures of a ballistic block in panel 2.2. point to a flight direction from NNE to SSW, suggesting the volcanic source in the north of the study area. Within the San Andrés Member the mean transport direction of the fluvial sediments was to the ESE with a circular standard deviation of 81°. In this member, a lava flow at the basis of section SO1 suggests a flow direction from W to E. Finally, the mean transport direction of the fluvial deposits of the Tepozteco Member was to the SSE (circular standard deviation 66°). However, in the stratigraphic sections SO, TO and the lower part of TL, dominated by the deposition of a

braided-river system, a palaeocurrent direction to the east is prevalent while in TEP, dominated by deposition from an alluvial fan, a N-S direction is prevalent. The sedimentary features in pyroclastic rocks within the Tepozteco Member have a mean transport direction to the south with a circular standard deviation of 37°, pointing to a source in the north.

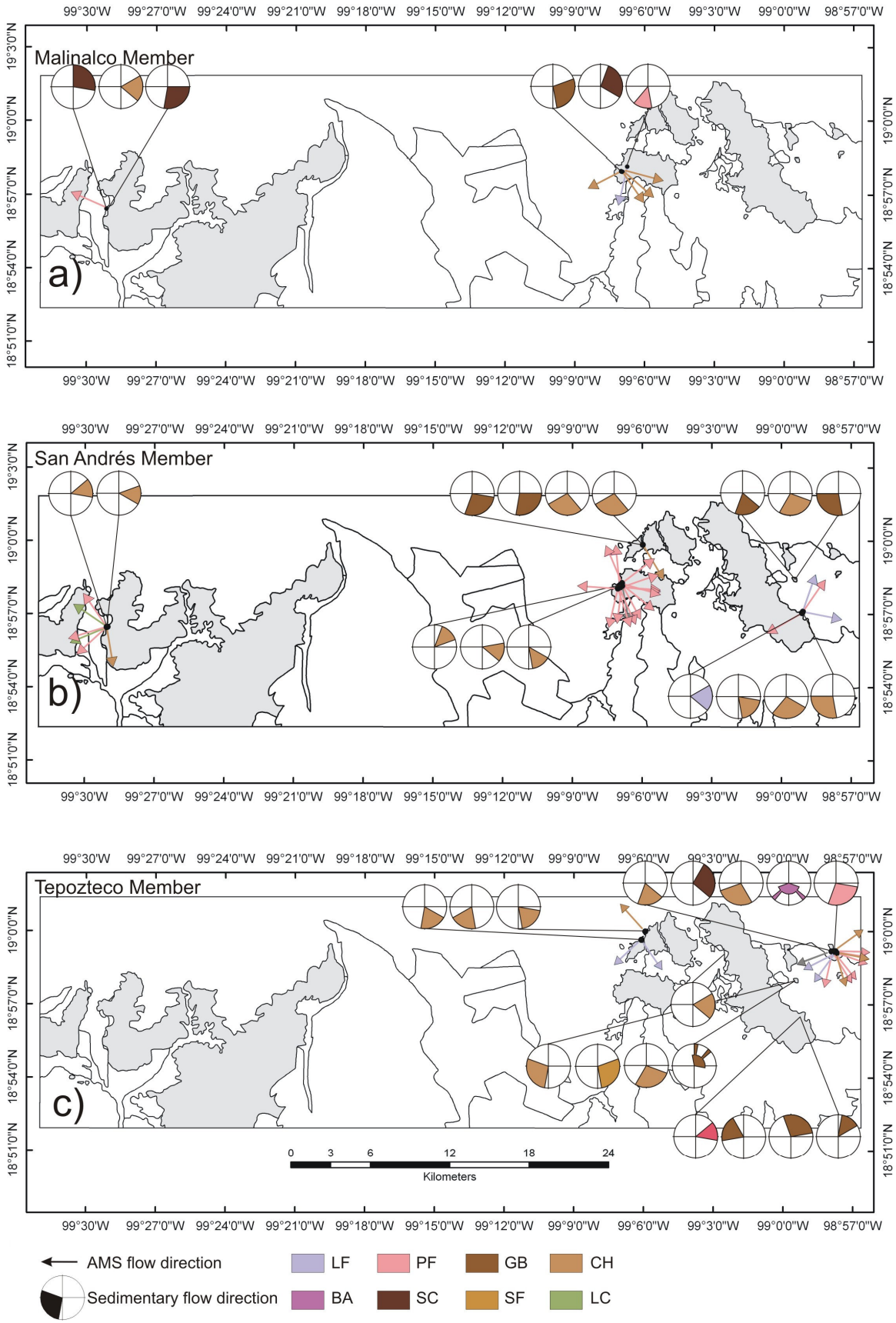

Figure 36. Palaeocurrent directions inferred from AMS analysis and sedimentary features. LF, Lava flow; BA, Block-and-ash flow; PF, Pyroclastic flow; SC, Scour pool-fill; GB, Gravel bar; SF, Sheet flood; CH, Channel-fill; LC, lacustrine. The colours of arrows correspond to depositional elements. The grey areas show the distribution of the Tepoztlán Formation.

Anisotropy of magnetic susceptibility (AMS) and magnetic fabric

The AMS depends on the anisotropy of each mineral grain and the spatial arrangement of the grains within the rock. It is thus a powerful indicator of the preferred orientation of minerals and provides information about the processes leading to the transport and deposition of pyroclastic rocks (Zanella et al., 1999). 428 samples were drilled with a gasoline-powered tool from 49 sites in the Tepoztlán Formation. At each site, cores were randomly distributed at different heights and over distances within a few meters. They were oriented with magnetic and solar compasses. One or two cylindrical, 2.2-cm long specimens were cut in the laboratory. The number of cores per site depends on outcrop condition, and varied from 5 to 28. The anisotropy of magnetic susceptibility was measured using an AGICO KLY3 Kappabridge. The AMS measurements are described by a second-order tensor with three principal eigenvectors $K1 \geq K2 \geq K3$ (Tarling and Hrouda, 1993). The following AMS parameters were used for this study: the mean susceptibility, $Km=(K1+K2+K3)/3$; the corrected degree of anisotropy, $P' = \exp \sqrt{\{2[(\eta_1-\eta)^2 + (\eta_2-\eta)^2 + (\eta_3-\eta)^2]\}}$ with $\eta = (\eta_1+\eta_2+\eta_3)/3$, $\eta_1 = \log K1$, $\eta_2 = \log K2$ and $\eta_3 = \log K3$ (Jelinek, 1981). The ellipticity of the susceptibility ellipsoid was expressed by the shape parameter T (Jelinek, 1981) defined by: $T = (2\eta_2-\eta_1-\eta_3)/(\eta_1-\eta_3)$ with $T>0$ for oblate magnetic susceptibility ellipsoids, and $T<0$ for prolate magnetic susceptibility ellipsoids. The principal eigenvectors (K1, K2, K3) of the mean normalized tensor and their confidence areas were calculated using the Jelinek method (Jelinek, 1978). The AMS parameters are listed in Table 7. The mean bulk susceptibility ranges from 1.05 to 9.77 x 10^{-3} SI. The anisotropy ratios are quite low with P' values between 1.004 and 1.214 (mean 1.034) but are within the range of usual values for volcanic rocks (e.g. Alva-Valdivia et al., 2005). Ellipsoids are all oblate ($0.016 \leq T \leq 0.667$). In most cases the axis with the highest degree of susceptibility (K1) corresponds to the long dimension of the grain whereas the direction of the least susceptibility (K3) corresponds to the short dimension. In this case, the magnetic fabric of titanomagnetite-bearing rocks mirrors the spatial distribution of non-equant grains, which lie with their largest dimensions within the magnetic foliation plane (normal to K3 axis) and the preferred orientation of the longest dimension parallel to the magnetic lineation (K1 axis). The maximum axis (K1) is normally interpreted as parallel to the flow direction and to represent an up-flow (sourceward-dipping) imbrication of the grains within the sample (Knight et al., 1986).

In most of the sites the K3 axes are tightly grouped and close to the vertical (Fig. 37); K1 and K2 are either grouped or more or less dispersed within the foliation plane, which is always close to the horizontal. The scatter of axes within the sites is ascribed to local turbulence of flow. The palaeocurrent directions, indicated by AMS fabrics, are shown in Fig. 36. At most sites, the azimuth of magnetic lineation is consistent with the direction of provenance as deduced from sedimentary features within the Tepoztlán Formation. Within the Malinalco Member, fluvial deposits show a prevailing flow direction to the SE, which is consistent with

measurements of sedimentary features in this area. The AMS fabrics of a lava flow show a southward flow direction, thus suggesting a source in the north. However, measurements on a pyroclastic flow in the west point to another volcanic source area in the south of the study area. The San Andrés Member shows a similar pattern in AMS fabrics like the Malinalco Member, especially regarding the pyroclastic flow deposits. Their flow directions validate the suggested volcanic sources in the SE and the N of the study area. Finally, the AMS measurements within the Tepozteco Member indicate two different point sources of volcanic material, north of Tepoztlán and north of the village San Agustín.

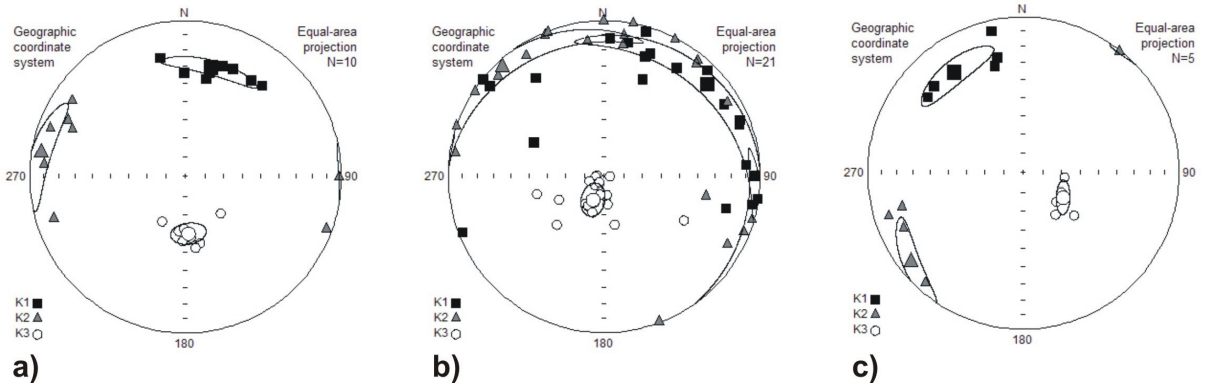

Figure 37. Examples for AMS fabrics from a) lava (flow direction from NNE), b) a pyroclastic flow (flow direction from NE) and c) a channel-fill (flow direction from NW).

Table 7: AMS data of the sampled locations.

sites	*n*	Km (10^{-3} SI)	K1 mean (Az./Incl.) [°]	Conf. angles K1 [°]	K2 mean (Az./Incl.) [°]	Conf. angles K2 [°]	K3 mean (Az./Incl.) [°]	Conf. angles K3 [°]	AMS parameters	
									P’	T
TL 1	**5**	6.8	69/24	41/18	320/36	43/13	185/44	22/18	1.031	0,295
TL 2	**5**	9.74	280/13	50/8	12/8	49/10	132/75	13/8	1.037	0,330
TL 4	**6**	5.69	13/10	65/19	281/10	65/10	147/75	19/12	1.034	0,303
TL 5	**5**	7.45	328/24	31/7	63/10	31/7	174/63	11/6	1.025	0,060
TL 7	**6**	9.10	289/20	17/6	20/4	24/13	120/69	22/6	1.052	0,043
TL 8	**8**	1.05	272/39	21/9	23/23	52/17	135/42	52/12	1.012	0,095
TL 9	**6**	7.05	321/11	33/11	228/14	33/13	88/72	16/9	1.015	0,608
TL10	**7**	1.21	343/26	34/19	253/1	34/20	162/64	24/21	1.009	0,390
TL11	**11**	5.88	36/30	25/19	129/5	47/19	228/59	48/16	1.018	0,316
TL12	**13**	5.37	63/42	51/15	255/47	51/12	158/6	17/10	1.058	0,184
TL13	**5**	3.14	234/1	28/7	325/31	29/5	143/59	11/6	1.032	0,211
TL14	**7**	2.81	282/23	14/7	17/12	8/4	134/64	13/4	1.050	0,143
SO1	**13**	5.97	281/28	62/14	188/6	62/26	87/61	28/15	1.060	0,602
SO2	**14**	5.64	215/3	41/23	305/1	41/30	42/87	31/24	1.023	0,200
SO3	**9**	2.45	60/12	27/10	150/1	27/8	242/78	10/9	1.029	0,317
SO6	**10**	1.76	199/7	33/4	295/42	33/13	102/47	13/3	1.214	0,642
SAC	**10**	2.63	13/29	23/4	279/7	23/7	177/60	9/6	1.038	0,667
SA4	**10**	4.54	286/31	39/20	58/48	39/17	179/25	26/21	1.023	0,110
SA5	**5**	6.21	7/36	31/11	240/39	29/12	122/30	20/12	1.050	0,216
SA6	**8**	6.63	349/34	28/14	239/28	28/12	119/44	17/11	1.044	0,413
SA7	**7**	6.29	157/2	38/4	247/9	37/17	52/81	18/4	1.043	0,627
SA8	**6**	6.70	233/24	44/9	345/41	44/14	121/40	18/10	1.010	0,301
SA10	**7**	5.19	332/17	53/11	241/4	53/15	237/73	19/9	1.015	0,414
SA11	**6**	5.17	174/1	29/3	264/39	29/21	83/51	21/7	1.018	0,389
SA13	**6**	6.43	13/62	39/21	263/10	39/12	168/25	23/7	1.023	0,366

SA15	**5**	6.58	342/37	18/6	94/26	27/9	210/41	27/14	1.042	0,278
SA16	**7**	2.14	277/62	33/10	11/2	33/4	103/23	11/3	1.025	0,343
SA17	**5**	3.47	251/45	32/12	354/12	35/18	95/43	27/9	1.077	0,622
SA18	**7**	5.13	274/40	38/8	7/3	38/8	101/50	11/8	1.018	0,311
SA19	**5**	3.59	336/28	52/9	219/40	52/15	90/37	17/13	1.016	0,167
SA20	**6**	3.88	94/63	64/25	315/21	63/14	219/16	29/15	1.013	0,484
SA21	**5**	5.59	309/11	36/15	217/9	35/8	91/75	22/8	1.019	0,317
SA23	**5**	5.72	325/23	20/7	232/9	20/6	122/66	9/4	1.076	0,358
SA24	**5**	6.71	310/13	37/15	44/16	37/11	184/69	15/13	1.014	0,320
SA25	**6**	5.01	63/4	50/6	333/3	51/6	203/85	9/3	1.009	0,515
SA26	**5**	4.68	284/14	22/9	188/24	22/16	43/62	16/9	1.004	0,148
TPO	**5**	5.38	329/17	54/11	239/2	53/10	144/73	14/10	1.016	0,205
TE9	**14**	5.42	133/22	54/24	41/4	55/30	301/68	35/24	1.018	0,016
TE10	**9**	7.30	325/64	27/8	160/25	19/9	67/6	31/8	1.027	0,072
TE11	**10**	4.59	47/9	13/5	313/26	19/5	154/62	16/5	1.022	0,137
TE12	**10**	6.32	138/3	36/35	46/22	68/36	236/68	68/33	1.014	0,298
MA 1	**16**	4.50	114/1	74/19	24/1	74/38	270/89	39/21	1.017	0,134
MA 2	**14**	6.20	146/5	37/10	54/18	42/36	252/71	41/11	1.011	0,076
MA 3	**24**	5.89	48/12	59/7	317/5	59/6	206/77	9/6	1.025	0,300
MA 4	**28**	9.35	124/18	55/19	33/2	54/13	299/72	30/11	1.012	0,355
MA 5	**13**	4.55	67/2	31/19	336/24	43/28	161/66	42/21	1.021	0,061
MA6	**7**	7.66	73/5	55/8	343/1	55/10	242/85	13/3	1.017	0,384
MA7	**12**	6.88	351/12	27/8	259/7	28/8	140/76	12/8	1.073	0,467
MA8	**10**	9.65	145/36	13/2	310/53	13/3	50/7	3/2	1.128	0,434

n = number of specimens measured. The mean susceptibility Km, the magnetic anisotropy P' and the shape parameter T are defined in the text.

Comparison between the palaeocurrent directions determinded from primary sedimentary structures and AMS data

The applicability of the anisotropy of magnetic susceptibility for the determination of palaeocurrent directions of a variety of deposits is already proved through various studies (Hillhouse and Wells, 1991; Palmer et al., 1996; Zanella et al., 1999; Zanella et al., 2001; Bascou et al., 2005; Alva-Valdivia et al., 2005). However, all these works only deal with one transport mechanism or deposit at a certain time. For this reason, the present study provides the possibility for a comparison of the quality of data, gained through AMS measurements on fluvial and pyroclastic deposits, and lava. As it can be expected, lava samples provide the lowest dispersion with average confidence angles of 33°/10° for K1, 36°/13° for K2 and 23°/9° for K3, providing the smallest confidence ellipsoids and thus giving the highest degree of reliability for the data. The reliability of AMS data from fluvial and pyroclastic deposits, however, do not coincide with the results provided by palaeomagnetic studies as described in chapter 3. Here, fluvial deposits show a lower dispersion (34°/13° for K1, 37°/13° for K2, 20°/12° for K3) than AMS samples from pyroclastic deposits (39°/11° for K1, 42°/14° for K2, 21°/10° for K3). This is due to the fact that AMS analyses measure an alignment of magnetic particles predominantly by transport processes and not necessarily an orientation by the geomagnetic field.

Primary sediment structures are still the most important features to derive palaeocurrent directions from sediments. They are relatively easy to recognize and to interpret and are relatively abundant in fluvial sediments. Within the study area, it was possible to document results from sedimentary features as well as AMS data from the same horizon (see sections SA1, TEP, SO1). Therefore, sedimentary structures could be used to calibrate the results from AMS data and to prove their reliability. Additionally, the comparison between flow textures in lava flows and AMS provided reliable information as well (see section SO1). The accuracy of AMS in pyroclastic rocks could partly be proved by their closeness to their suspected source areas (see sections MA, SA1, TL). Contradictions between the data of closely related fluvial strata can be explained either by a channel shifting or the meeting of two different river systems with E-W axial and a divergent flow direction (see section SA1). In case of lava and pyroclastic flows, however, contradictions in flow directions can be explained by pinching lobes (see section SO1), displaying changing directions in median to distal distances from their source areas.

4.3. Discussion and depositional model

The vertical and lateral analysis of individual depositional elements and their distribution within the study area, as well as information gained during mapping in the field and outside the stratigraphic sections, can be integrated in three depositional models, forming a concise evolutionary model of the Tepoztlán Formation (Fig. 38-40), and illustrating their importance for the interpretation of the succession. The facies patterns within the stratigraphic sections record temporal changes in sedimentation, showing syn- and inter-eruptive sedimentation as indicated by fluvial, mass flow and primary volcanic depositional processes. The interpretation of these facies patterns reveals a post-eruptive volcaniclastic re-sedimentation in a fluvial environment, intertwining with sedimentation from a volcanic induced alluvial-fan during and in the aftermath of explosive eruptions. The volcanic activity, combined with syndepositional tectonics, were the main controlling factors in alluvial sedimentation. During episodes of increasing sediment supply by volcanic activity, a progradation of the fans was recorded and coarsening-upward trends developed.

The locations of volcanic edifices were deduced either through direct observations in the field or indirectly, based on the average runout distance of certain deposits as stated by Williams and McBirney (1979) and Einsele (2000) and by means of palaeocurrent and AMS measurements. The scale of the volcanoes is considered to be schematic. Locations that could not be identified either in the field or by means of AMS measurements and average runout-distances are marked with a question mark within the sketches. However, their existence is deduced from volcanic material that could not be assigned to one of the formerly described edifices, either due to too long runout distances or an assumed start of volcanism of an edifice

that could only clearly be proved in a following member. Furthermore the course of the braided-river system outside the documented and measured stratigraphic sections is considered to be more or less schematic. Inflows from the north are supposed to have been present at that time, considering that the Valley of Mexico was drained to the south (Ochoterena, 1978), but could not be identified in the field.

Once the depositional elements and their distribution had been identified, analysed and interpreted, and the palaeocurrent directions had been investigated, three distinct palaeoenvironmental settings could be deduced, characterised by the three members of the Tepoztlán Formation during the Lower Miocene: (1) the Malinalco Member, a setting dominated by the deposition from a braided river system, (2) the San Andrés Member, a setting dominated by volcanic edifice development, and (3) the Tepozteco Member, a setting dominated by volcanic edifice destruction.

Braided river setting (Malinalco Member, 22.8 - 22.2 Ma)

The studies on sedimentary features and palaeocurrent directions show, that a W-E trending braided river system was dominating within the study area between 22.8 and 22.2 Ma. The fluvial sediments, mostly gravel bars and sandy channel-fills, were predominantly deposited near Malinalco, Ahuatenco and San Andrés. Vertical stacking of sand and gravel bodies are interpreted to be due to aggradation with shifting of channel bars associated with channel switching (e.g. Bridge, 1993). The complete lack of paleosols and non-volcanic clasts gives evidence for a highly active system with frequent eruptive activity and immediate subsequent reworking and resedimentation. The abundant eruptions supplied relatively small to moderate rock volumes from still small volcanic edifices running along the southern and northern edge of the axial fluvial system. SE of Malinalco a volcanic centre of this time could be identified by vent breccias and radial dykes (18.52°N, 99.24°W). The AMS measurements on pyroclastic flows in Malinalco are consistent with this source region (see Lenhardt et al., in prep.). According to palaeocurrent data another centre must have existed in the area of the present day Sierra Chichinautzin, north of Tepoztlán.

Following the eruptions, large volumes of volcaniclastic debris were reworked from proximal areas and discharged into the basin. This resulted in the development of a low-sinuosity channel system with high-sediment-laden hyperconcentrated flows after heavy rains. The prevalence of intermediate clasts and their relatively large sizes are consistent with a limited distance from the source via a high-energy transport system and thus suggest contemporaneous volcanism and sedimentation. The overall coarsening- and thickening-upward trend, together with an increase in average grain size, can be attributed to a steepening of the relief and the progradation of large fan lobes of a volcanic induced alluvial fan into the

river basin (e.g. Clemente and Perez-Arlucea, 1993; Horton and DeCelles, 2001; Uba et al., 2005).

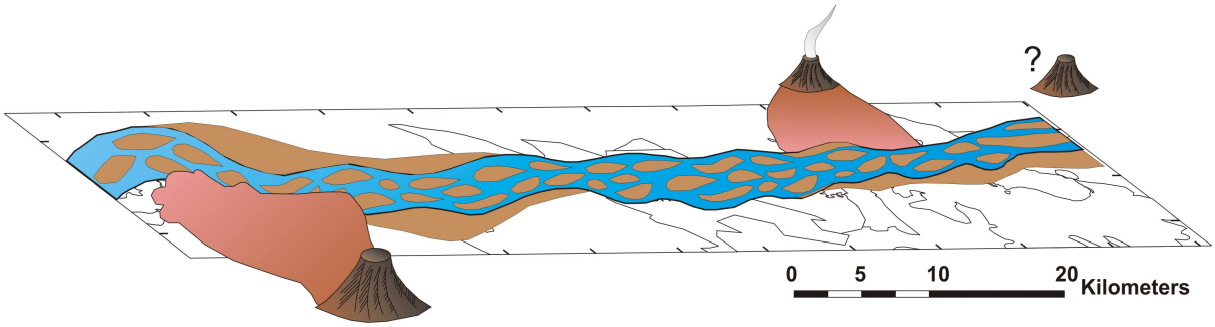

Figure 38. Palaeoenvironmental reconstruction of the braided river setting (Malinalco Member, 22.8 - 22.2 Ma).

Volcanic edifice construction (San Andrés Member, 22.2 - 21.3 Ma)

During the deposition of the San Andrés Member a further progradation of the volcanic system is recognized, combined with a sudden increase in volcanic activity which is associated with the deposition of massive ignimbrites and the most voluminous lava flows of the Tepoztlán Formation. Regionally, the thickest ignimbrites can be found near San Andrés (up to 30 m) while thick lava flows are prevalent in the vicinity of Tlayacapan and Ahuatenco (up to 400 m). AMS measurements on the ignimbrites suggest a point source in the north. Thin pyroclastic products, with a supposed source in the north, are also found in Malinalco but can not be assigned to the source near San Andrés due to too long runout distances. Thus, another volcanic source is suggested to have existed close to the present day Zempoala region. This is in accordance with De Cserna and Fries (1981), who thought this region to be one of the source areas of the Tepoztlán Formation in Malinalco. The Zempoala volcanic region is furthermore supposed to be the source of massive the lava flows which can be found near the village of Ahuatenco in the State of Mexico (18.56°N, 99.19°W). Dating revealed, that the thickest lava flows of the Tepoztlán Formation occur in this region at this time (K/Ar ages of 22.4 ± 0.5 Ma, 21.9 ± 0.5 Ma; Lenhardt et al., submitted). The lava flowed southward into a pre-existing depression cut into the sedimentary sequence (Lehmann, 2009; Faridfar, 2009; Cizmezcia, in prep.).

In Malinalco, the formerly described pyroclastic deposits intertwine with pyroclastic flow deposits which are interpreted to originate from the volcanic edifice in the south. However, in general this locality is dominated by thick horizons of gravel bars and sandy channel-fills, indicating the on-going sedimentation of the axial braided river system. Lacustrine sediments found in Malinalco and near the village of Santo Domingo point to the development of lahar-dammed lakes after partial covering of the former river bed by volcanic activity and a ponding

of the water in the newly formed sedimentary basin. In San Andrés, the pre-existing fluvial system was partly covered or diverted by volcanic deposits and could only follow its original course in times of quiescence, as indicated by thin fluvial sediments within the thick sheets of ignimbrites. In the beginning, pyroclastic flows filled up the existing fluvial channels, explaining their lense-shaped appearance. Later, primary deposits have a sheet-like appearance, covering and modifying the palaeotopography and leading to further steepening of the relief in the context of the growing alluvial fan in the north.

Explosive eruptions (volcanian to sub-plinian) from small volcanoes, causing the deposition of pyroclastic flows and subordinate surge deposits, were accompanied by few effusive episodes. The volcanian to subplinian events generated only few ash falls and relatively small pyroclastic density currents, probably extending not more than a few kilometres from their vents. Although initial plinian eruption clouds may have developed, they would have been short-lived and collapsed early into an ash and debris fountain, which fed pyroclastic flows onto the outer slopes. This may explain the existence of only few fall deposits (e.g. White and Robinson, 1992). The deposits from block-and-ash flows and lava point to proximal small vents near San Andrés and Tlayacapan. The top of the San Andrés Member is characterised by an increasing influence of the alluvial fan in the north, indicated by an increase in lahars.

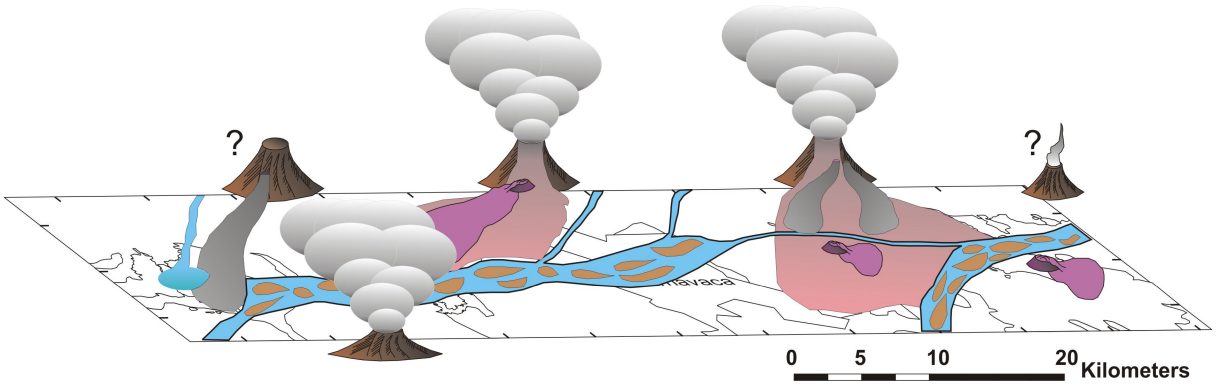

Figure 39. Palaeoenvironmental reconstruction of the volcanic edifice construction (San Andrés Member, 22.2 - 21.3 Ma)

Volcanic edifice destruction (Tepozteco Member, 21.3 - 18.8 Ma)

The deposition of the Tepozteco Member is characterized by a prevalent sedimentation in the eastern part of the study area (Tepoztlán and Tlayacapan region) and is missing in the Malinalco and Ahuatenco region (see Fig. 2). Deposition in the west, i.e. the Malinalco area, seems to have ceased during that time. This is either due to a shifting of the initial braided river system during that time or a later erosion of younger sediments. However, in the other parts of the Tepoztlán Formation deposition of the braided river system was still prevailing.

Nevertheless, the palaeocurrent analysis in the study area indicates that basin sedimentation underwent a significant change from a W-E trending fluvial to a N-S trending mass flow deposition. The influence of the alluvial fan system in the north of the study area, which could already be observed within the San Andrés Member, is increasing and overcomes the formerly dominant axial system during this period. This can especially be seen within the TEP section which is interpreted as the active part of the volcanic induced alluvial fan, presumably developing at the southern edge of a prominent volcanic edifice with an estimated altitude clearly exceeding 3000 m a.s.l. This volcano complex underwent edifice destruction generating various types of debris flow deposits. The increase in sediment supply, associated with high rates of lahar activity resulted in an aggradation in stream valleys and on aprons surrounding the volcanic edifice (e.g. Vessel and Davies, 1981; Scott, 1985; Smith, 1987).

From palaeocurrent analysis and proximity of depositional units the former centre of the stratovolcano responsible for the Tepozteco Member must be buried below the modern lava flows of the Sierra Chichinautzin. Clast compositions and lithologies indicate that the entire material was locally derived. Deposits originating from debris flows are inferred to have been produced by relatively near-source reworking of block-and-ash or pumice-and-ash flows. The appearance of pyroclastic surges, few pumice fall layers and intermediate lava flows or domes in section TEP, respectively, support this hypothesis. The association of thick lavas (up to 20 m), autoclastic and pyroclastic breccias, and bouldery lahar deposits as it can be seen in section TEP is common on the flanks of stratovolcanoes and characterise many proximal to median apron settings (e.g. Hacket and Houghton, 1989, Vessel and Davies, 1981, Mack and Rasmussen, 1984).

The lahars flowed southward from their source area and spread over the braided stream valley, leading to a partial covering or southward shift of the initial braided river system. The major periods of apron construction occurred during eruptive periods, characterised by the deposition of mass flows or primary volcanic products. The tabular debris flow deposits indicate that they were too large to be contained by the channels. Periods of quiescence or reduced volcanic activity are characterized by reworking and erosion of eruption-related deposits (e.g. Palmer and Walton, 1990), resulting in the deposition of sandy to gravely fluvial deposits. Gravel bars, deposited during these periods, indicate the existence of high-magnitude floods. The development of soils could be not observed. Instead pollen findings in the matrix of the lahars indicate the existence of forest vegetation outside the main active areas.

Throughout the section TEP, primary volcaniclastic products are decreasing and are absent in the upper third of the section while debris flow deposits are increasing in number and thickness. This either suggests a time of inactivity or a growth of the volcanic vent to an altitude from where primary volcaniclastic products could not reach the place of deposition in section TEP anymore. However, the latter hypothesis is favoured. Therefore, a lava flow in

the upper part of TEP and at TL is interpreted to be due to a parasitic vent at the southern flank of the large stratovolcano which existed at the present location of the Sierra Chichinautzin.

In contrast to the central part of the study area around Tepoztlán, the parts to the east (SO1, SO2, TO) were not or only partially affected by deposition from the alluvial fan, showing a marginal setting. Especially the deposition of abundant sheet floods is a sign for floodplain sedimentation in marginal areas of the fan (e.g. Luzón, 2005) or at the alluvial fan front, i.e. at the transition to the river system. The dominance of channel-fill and gravel bar elements indicate a continuation of the braided-river system in these areas, whose fluvial transport is occasionally disrupted by explosive eruptions in the near surrounding and highly supplied with pyroclastic material.

The deposition near San Agustín was influenced by another volcanic centre very close to the section itself but also presently covered by lavas of the Chichinautzin Formation. Chronostratigraphic correlations point to a synchronous activity to the upper Tepozteco member and hence, Section TL is characterised by massive ignimbrites and a lava dome on top of the section, emphasizing the proximity to the vent area. Palaeocurrent data on these ignimbrites suggest the volcanic edifice to have been N to NE from the studied section. We interpreter these volcanic products as coming from a lateral vent at the south-eastern flank of the large stratovolcano, which had reached a critical height at this time in terms of slope failures and the uprise of lava.

Finally, the emplacement of dykes within the Tepoztlán Formation (15.83 ± 1.31 Ma; Lenhardt, 2004) is related to a period of plutonic to subvolcanic body emplacement and large fissure eruptions with widespread lava plateaus between the states of Nayarit and Veracruz (Ferrari and Rosas-Elguera, 2000; Ferrari, 2004; Ferrari et al., 2005).

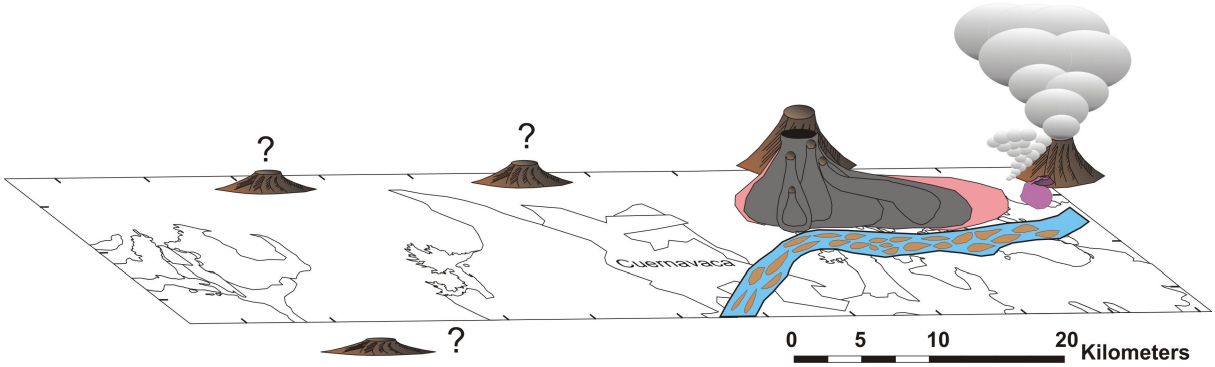

Figure 40. Palaeoenvironmental reconstruction of the volcanic edifice destruction (Tepozteco Member, 21.3 - 18.8 Ma).